IGC Newsletter

IN THIS ISSUE

From the Editor

Dear Reader

It is my pleasure to wish you a very happy and pleasant New Year 2013.

It is my pleasant privilege to forward a copy of the latest issue of IGC Newsletter (Volume 95, January 2013, issue).

In the Director's Desk, Shri S. C. Chetal, Director, IGCAR has highlighted the emphasis on improved economics and enhanced safety in the design of twin units of 500 MWe Fast Breeder Reactors planned to be constructed in the near future.

In the first technical article Dr. C. Phaniraj and colleagues, have proposed a new relationship between the two stress multipliers, in terms of stress component (n_p) for the data obtained from hot compression tests on modified 9Cr-1Mo (P91) steel over a wide range of strain rates and temperatures. In the second technical article, Shri K. K. Kuriakose and his colleagues have brought out the critical features in the design, development and commissioning of the electrical sub-system for PFBR Operator Training Simulator that is used for training and certifying power plant operators.

In the young officer's forum, Shri Govind Kumar Mishra has shared his experience in the construction and commissioning of integrated top shield test facility, towards the design of top shield. Shri Karuna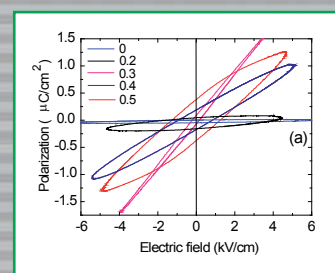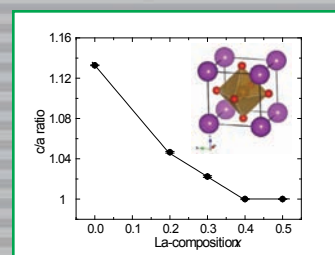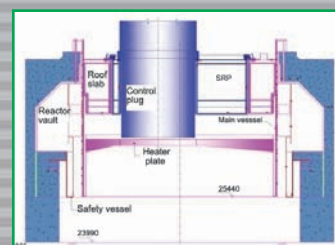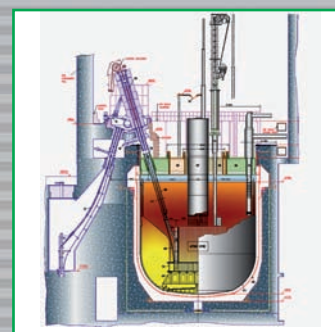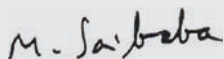 Kara Mishra, in the young researcher's forum has studied the structural, vibrational, dielectric and magnetic properties of multiferroic La-substituted $BiFeO_3$-$PbTiO_3$. This newsletter carries reports on the "11th International Conference on High Nitrogen Steels and Interstitial Alloys, Theme meeting on "Structure and Thermodynamics of Emerging Materials", "Supercritical Fluids" and "National Symposium on Radiation Physics" .

A delegation from United States Nuclear Regulatory Commission (USNRC), USA, Prof. Vijay Sazawal, Director of Government Programs at USEC, Inc, USA and Shri Ashok Lavasa, IAS, Additional Secretary (Power), Ministry of Power visited the Centre during the last quarter.

We are happy to share with you the awards, honours and distinctions earned by our colleagues. We look forward to your comments, continued guidance and support.

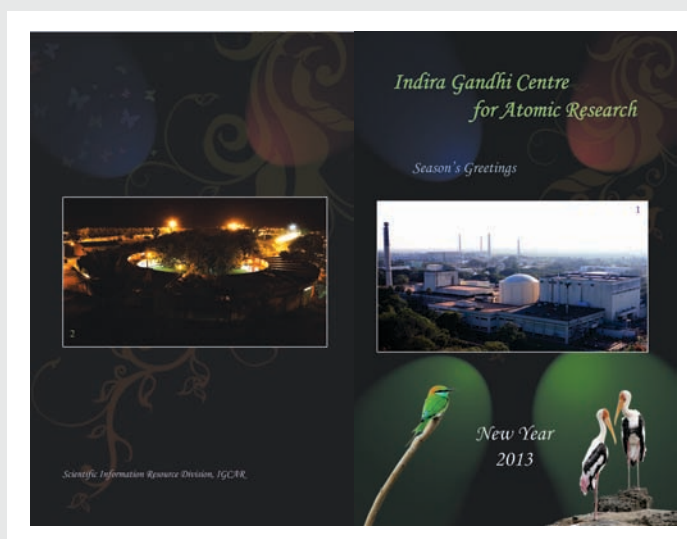With my best wishes and personal regards,

M. Sai baba

(M. Sai Baba)
Chairman, Editorial Committee, IGC Newsletter
&
Associate Director, Resources Management Group

Director's Desk

Beyond PFBR to FBR 1 and 2

In the Indian energy scenario projections for the future, nuclear power through fast reactors has been considered as an important component. Fast reactors are also planned to be built in the medium term to burn minor actinides as means of reducing the burden of radioactive waste management. 500 MWe Prototype Fast Breeder Reactor (PFBR), the first indigenously designed fast reactor, is now in an advanced stage of construction at Kalpakkam.

The design features of PFBR were selected based on the available technology and its maturity at the time of design. In the reactor assembly, box type structure is chosen for the top shield consisting of roof slab and rotatable plugs from engineering considerations. The reactor assembly is supported at the top and sufficient gap is provided between safety vessel and the reactor vault with the idea of possible access to the area. The inner vessel is made of two cylindrical shells connected by conical redan. Two

primary pumps are connected to grid plate with two primary pipes on either side and the grid plate has sleeves bolted to top and bottom plates for supporting all the core sub-assemblies. The above mentioned major features are shown in the vertical section of PFBR reactor assembly in Figure 1.

The fuel handling scheme is through two rotatable plugs and one transfer arm type machine for in-vessel handling and inclined fuel transfer machine for handling between in-vessel and ex-vessel as shown in Figure 2.

The primary sodium purification circuit is ex-vessel. The steam generators are once through type having twenty three metre long tubes with expansion bend.

Design activities for two more 500 MWe Fast Breeder Reactors (FBR 1 & 2) with improved economics and enhanced safety features, adopting a twin unit concept (2x500 MWe), are in
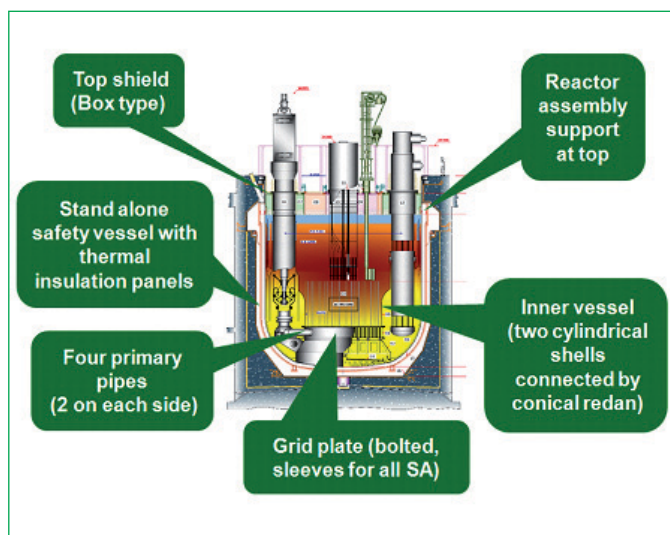

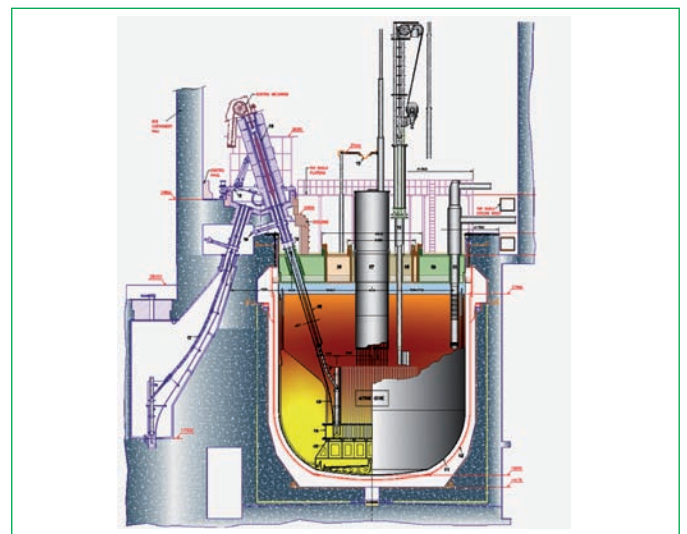Figure 1: PFBR reactor assembly features

Figure 2: Ex-vessel fuel handling

progress at our Centre. These reactors will be constructed adjacent to PFBR. The major features of PFBR which have undergone design improvements in the future FBR 1&2 are briefly described below.

With the objective of demonstrating the potential of FBRs, the matured fuel cycle technology with mixed oxide fuel that was adopted for PFBR, is retained. Further, for PFBR, two loop concepts with two primary pumps, two intermediate heat exchangers per loop and two secondary sodium pumps were selected, after considering comprehensively the associated parameters such as economics, plant availability, size and number of components, fast reactor operating experience, capacity and capability of Indian industries and safety aspects. In view of these, the cost of the secondary sodium circuit has been kept as low as possible and hence, there is little scope for further reduction in the cost for the secondary sodium circuit except for the steam generators. However, use of twin unit concept for sharing non safety systems, use of advanced shielding materials such as ferro-boron, SS304LN in place of SS316LN for cold pool components and Cr-Mo steels for secondary sodium piping, three steam generator modules per loop with increased tube length of thirty metres (PFBR has four modules per loop with twenty three metres length as shown in Figure 3) enhancing the design life from 40 to 60 years and target peak burn-up to 150 GWd/t (against 100 GWd/t for PFBR) have indicated significant reduction in the capital cost and tariff. Burn-up increase is through change of cladding and wrapper material from 20% cold worked 15Cr-15Ni+Mo+Ti (D9) employed in PFBR to 20% cold worked modified D9 with further control of tramp elements for cladding and 9Cr-1Mo wrapper for FBR 1&2. Apart from the features mentioned above, construction

experience of reactor assembly components indicates a need for major improvements in the design of grid plate (large number of sleeves, posing challenges in assembly, hard facing of large diameter plates and heavy flange construction), roof slab (large welded box type structure with risk of lamellar tearing and long manufacturing time, inclined fuel transfer machine (long manufacturing time and extensive qualification tests), unduly large gap between safety vessel and reactor vault and long time delay in view of the import of large diameter bearings. To take into account these feedbacks for the future design, improvements have been conceived in the reactor assembly as shown in Figure. 4

(1) reduction of main vessel diameter

(2) dome shaped roof slab with conical support skirt under compression

(3) thick plate concept for the rotatable plugs

(4) welded grid plate with reduced number of sleeves, reduced diameter of intermediate shell and reduced height

(5) increased number of primary pipes

(6) inner vessel with single radius torus welded with the grid plate

(7) integrated liner and safety vessel with thermal insulation arrangement and

(8) optimization of main vessel, inner vessel and safety vessel thickness

These apart, fuel handling system has been simplified. These improvements have brought significant cost benefit with enhanced
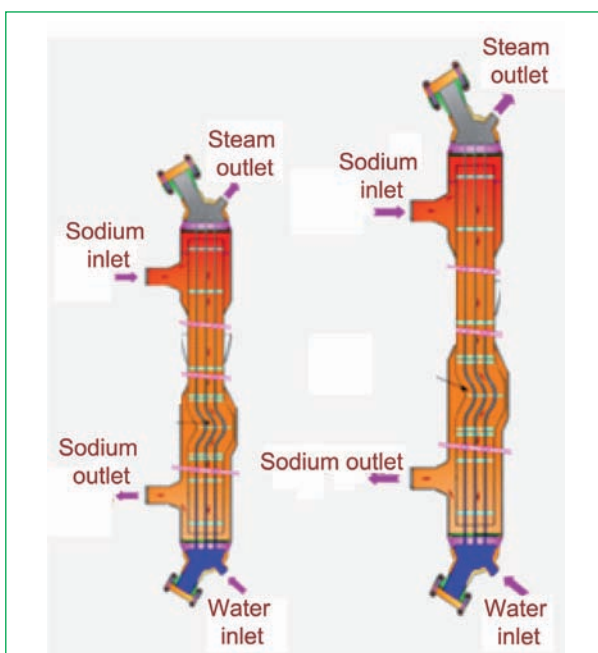

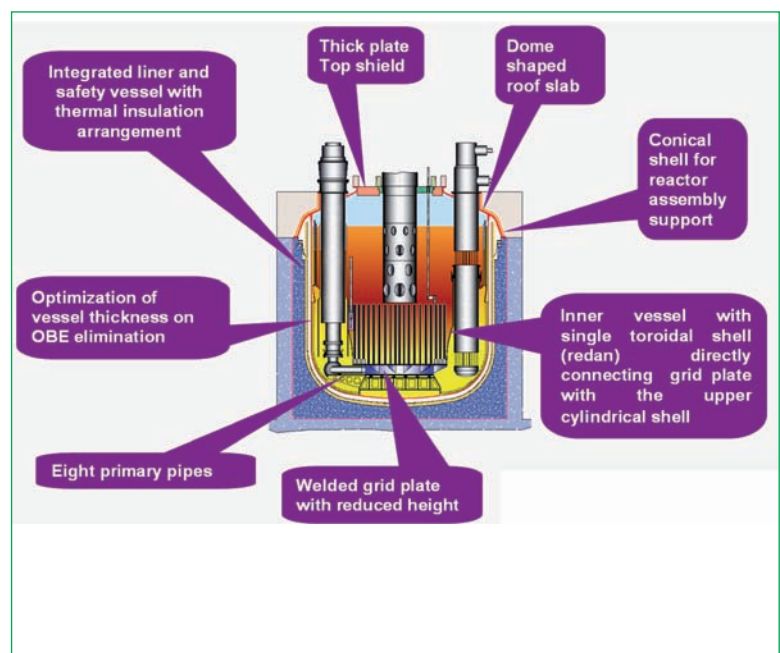Figure 3: Steam generators

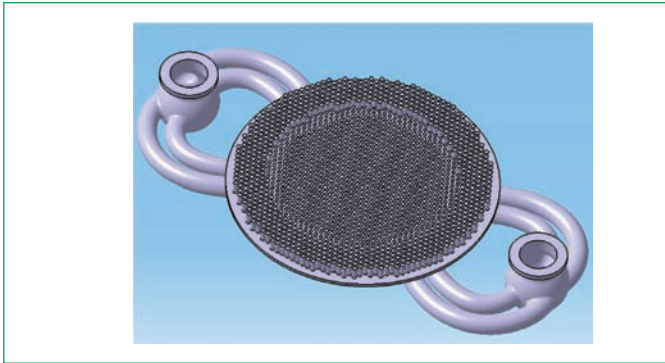Figure 4: Major improvements introduced in the CFBR reactor assembly
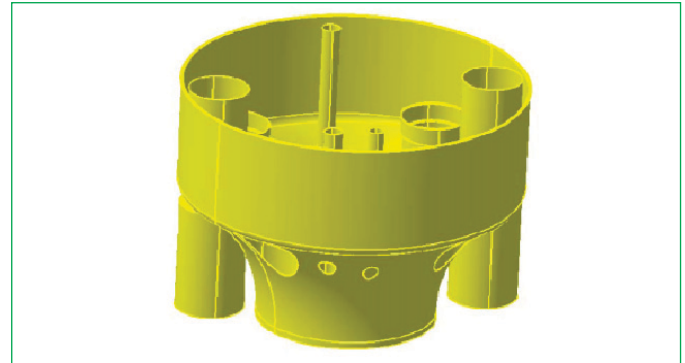
Figure 5: Primary pipes and grid plate

Figure 7: Inner vessel with single torus

safety. The technical basis of these changes is elaborated below.

Reactor Assembly Components

Main vessel diameter is an important parameter that quantifies the improvements of the reactor assembly. The radial spacing at core level as well as at the top shield level and the circumferential spacing at the top shield level decide the vessel diameter. The use of integral control plug with small rotatable plug, reduction of the gaps between the flanges in view of different levels of flanges taking the advantage of the dome shaped roof slab, machining of penetration shells in roof slab and reduction in the annular gaps between inner vessel and thermal baffles and thermal baffle and main vessel based on the experience gained from manufacturing of components of PFBR leads to the reduction of main vessel diameter from 12.9 to 12.1 metres.

In PFBR, as per one of the safety studies, it is seen that the core flow reduces to 30% under one pipe rupture case. To increase the safety margin in FBR 1&2, eight pipes are provided, i.e. four per pump, thereby reducing the diameter of pipes from 630 to 455 mm. The increased number of pipes increases the safety margin due to pipe rupture event, i.e. the (core flow is 57% of nominal flow) and maximum clad hot spot temperature is reduced by $\sim 230^{\circ}$C. The layout of the pipes is optimised, taking the advantage of additional space gained through adopting reduced cold plenum volume in the welded grid plate concept (Figure 5).

In PFBR, out of 1758 sleeves in the grid plate, 732 sleeves support and facilitate coolant flow for fuel, blanket, reflectors, inner B_4C, absorber rod and storage sub-assemblies and the remaining 1026 sleeves are incorporated to support shielding sub-assemblies, which do not require any coolant flow. In order to simplify the design, the coolant plenum is reduced by accommodating only 732 sleeves that are needed for facilitating the coolant flow. In addition, 197 sleeves without holes are incorporated for shielding sub-assemblies for achieving uniform flow distributions in the grid plate. The remaining sleeves are eliminated, spigots are welded to the grid plate top plate to support the shielding sub-assemblies, which are not to be replaced during the entire plant life. This results in reduction of diameter of the intermediate shell to 3.9 metres, while the top plate diameter is retained as 6.1 metres. This reduction of cold plenum in grid plate facilitates comfortable layout for the eight primary pipes. Further, in the revised grid plate concept, welded joints are conceived between the shell-to-plates and sleeves-to-plates, instead of bolted joints. Welded joints are preferable from manufacturing, better thermo-mechanical and economic considerations. Appropriate heat treatment would be carried out for the dimensional stability of welded grid plate. In view of reduced diameter of primary pipes, the height of grid plate is reduced accordingly, i.e. 685 mm as against 1000 mm for PFBR. The net weight reduction of new grid plate is estimated as 55%. It is estimated that the welded grid plate would result in cost saving of about 30%, compared to bolted design of PFBR. Figure 6 depicts the welded grid plate with eight primary pipes.

Regarding inner vessel, the redan, which connects the top and bottom cylindrical shells is changed to single toroidal shell due to its inherent higher buckling strength. Stress analysis indicates that this new geometry calls for reduced thickness, i.e. 15 mm instead of 20 mm (Figure 7). The new shape can accommodate in-vessel transfer port (IVTP), which was in the grid plate of PFBR. By transferring the port from grid plate to inner vessel, the core layout is made symmetrical in the grid plate.
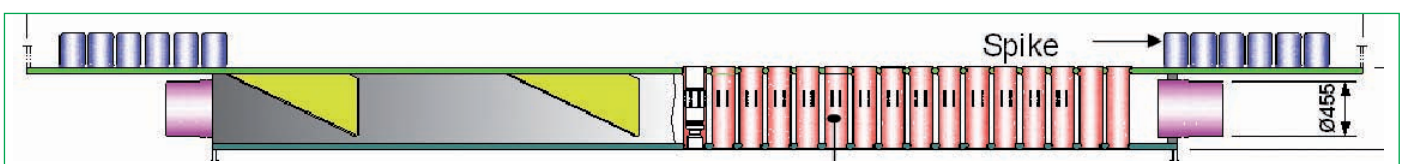

Figure 6: Welded grid plate

Figure 8: Dome shaped roof slab and thick plate concept for rotatable plugs

Figure 9: Embedded safety vessel

The large box type structure with many penetrations, made of carbon steel posed a lot of difficulties during manufacturing, in particular due to lamellar tearing and found to be time consuming, in PFBR. Alternatively, taking the advantages of higher load carrying capacity with possibly minimum thickness, a dome shaped roof slab is conceived which comprises a conical shell connected to vertical shell through short torus portion. Material of construction for the shell is chosen as SS304LN to avoid the bi-metallic joint. The triple point junction has to be machined from forged piece. Through machining of the large rotatable plug shell with a stepped geometry, it is possible to have minimum annular gaps, which helps to reduce the complementary shielding requirements on the top shield, achieve minimum main vessel diameter and also mitigate the sodium ejection through the annular gap under core disruptive accident. In line with the dome shaped roof slab, the rotatable plugs are conceived from thick plates with

their outer flanges machined from thicker forged rings. Figure 8 depicts the concepts adopted for roof slab and rotatable plugs.

While the concepts of inner and outer walls of the reactor vault adopted for PFBR are retained, a few important changes are proposed for the safety vessel. The material of construction is changed from SS304LN to carbon steel. This is justified by ensuring that the temperature of leaked sodium and thereby safety vessel temperature would not lead to significant creep in view of reliable and dedicated safety grade decay heat removal exchangers immersed in the hot pool. The annular radial gap of 250 mm, which is provided between the safety vessel and inner reactor vault for PFBR, is eliminated. To enhance the strength of the vessel, in particular during the seismic events when main vessel is under leaked condition, studs would be incorporated by welding one end with safety vessel and another end close to the inner wall surface. The required space between the stud end

Figure 10: Revised fuel handling scheme

Figure 11: Major components that have undergone technology development exercise are (1) tri-junction forging for dome shaped roof slab, (2) large diameter bearing, (3) thick plate welding for rotatable plugs, (4) welded grid plate and (5) inner vessel with redan of large single torus

and inner wall is optimized based on thermal expansion of safety vessel, which needs to be accommodated and the allowable displacements of the vessel during seismic events. Thermal insulation panels provided in PFBR design would be retained. Figure 9 shows the integration of safety vessel with the reactor vault.
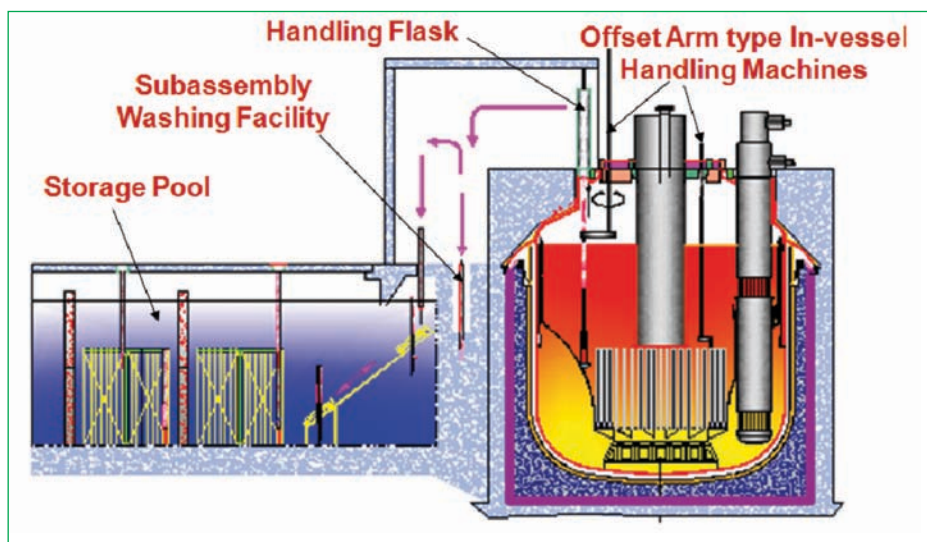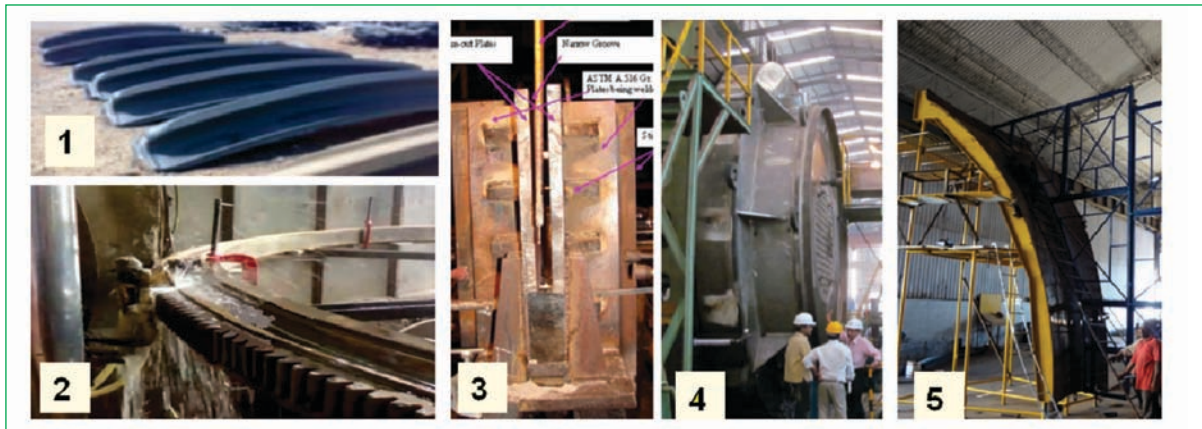
Fuel handling system

Construction experience of PFBR indicated that it is preferred to adopt a simplified fuel handling system. Hence, the fuel handling scheme is revised by eliminating the inclined fuel transfer machine. Instead, a straight pull machine is proposed to transfer the sub-assembly between storage location to the in-vessel transfer port, which is located in inner vessel lower portion. The transfer of sub-assembly between the respective location in the core and in-vessel transfer port are achieved through two transfer arms as indicated in the Figure 10.

Reduced component wall thickness

For PFBR, design has been done for both operating basis earthquake and safe shut down earthquake. For non-inspectable components, the allowable stresses are based on normal operation limits. The minimum wall thickness of various shells in the reactor assembly has been governed by the operating basis earthquake. The peak ground acceleration which is twice the value of operating basis earthquake, is not deciding the wall thickness in view of higher damping, for safe shutdown during earthquake. It is proposed to make operating basis earthquake as inspectable earthquake with a gross check for 1/3rd value of safe shutdown earthquake. In terms of material savings, the thickness of main vessel can be reduced to 20 mm, from 25 mm through elimination of operating basis earthquake in design.

The modified design of reactor assembly results in savings of specific stainless steel requirements (tonnes/MWe) by ~22%.

Technology Development Exercise

Technology development exercises have been completed for the components shown in Figure 11. In addition production of thirty metres long modified 9Cr-1Mo steam generator tube is under progress.

Future Directions

The capital cost reduction, reduced construction time, reduced depreciation due to longer design life, reduced O&M cost due to co-location of two units, as well as reduction in fuel cycle cost due to increased burn-up gives confidence of improved economics. Adoption of in-vessel primary sodium purifications, increased number of primary sodium pipes, passive diverse shut down system, incorporation of third shut down system, longer steam generator tubes, modified decay heat removal system of six circuits based on combination of passive and active system with the active system capable of 60% heat removal by natural convection leads to enhanced safety. R&D road map has been well laid with emphasis of indigenous development. Lessons learnt from construction of PFBR as well as Indian PHWRs will provide means to reduce construction time for FBR 1&2. Manufacturing of long delivery components under a consortium of multiple industries could be worth pursuing. Indian industries have demonstrated their expertise in manufacturing PFBR components to stringent tolerances, what is needed for FBR 1&2 is reduced manufacturing time by the Indian industry. Reduction in construction time of FBR 1&2 will be important to demonstrate the economic competitiveness of FBRs.

S. C. Chetal
Director

A New Relationship for Constitutive Analysis in Hot Deformation for Modified 9Cr–1Mo (P91) Steel

The simulation of metal forming processes using finite element analysis relies on the accurate knowledge of hot deformation behavior as influenced by the process parameters. Hot compression tests are widely employed in evaluating the hot working behavior of materials since uniform deformation can be attained even at high strain rates as those encountered in industrial practice. True stress–true plastic strain data obtained from uni–axial compression tests at various strain rates and temperatures are described in terms of suitable constitutive equations that adequately correlate flow stress, strain rate and temperature. The merit of these equations depends on how accurately they predict the flow stress under varying processing conditions. The power–law description between flow stress and strain rate, which is preferred for creep is suitable at low stresses/ strain rates, while the exponential relationship is valid at high stresses/strain rates. Though the exponential law was initially favored for hot working processes, it has the inadequacy that it breaks down at higher temperatures and lower strain rates. The most widely accepted constitutive equation in the hot working domain is the Garofalo hyperbolic–sine expression with Arrhenius term which relates flow stress (σ), strain rate ($\dot{\varepsilon}$) and temperature (T), and is given as

$$\dot{\varepsilon} = A_g [\sinh(\alpha_g \sigma)]^{n_g} \ e^{-Q/RT} \qquad (1)$$

where Q is the apparent activation energy, A_g, n_g and α_g are constants and this relation is valid for the entire strain rate/ stress regime. The above equation suitably correlates the stress dependence for the entire stress regime, as it reduces to power– law at low stresses (valid for $\alpha_g \sigma < 0.8$) and exponential at higher stress limits (applicable for $\alpha_g \sigma > 1.2$).

The determination of stress multiplier (α) is crucial for constitutive analysis in hot working. It is necessary to realize that during creep conditions, as strain rate is a derived quantity, the power–law stress exponent 'n' at lower/intermediate stresses i.e.,

$$\dot{\varepsilon}_S = A^{/} \sigma^n e^{-Q/RT}$$

and similarly β in the high stress region i.e.,

$$\dot{\varepsilon}_S = A^{//} \ e^{(\beta\sigma)} e^{-Q/RT}$$

are distinctly obtained which allows clearly the determination of α (i.e. α = β/n) in the Garofalo equation that suitably describes the stress dependence of steady state creep rate $\dot{\varepsilon}_s$ for the entire

stress regime. On the other hand, the situation during hot working is different where strain rate is imposed and the flow stress data is force fitted by plotting $\ln(\dot{\varepsilon})$ vs. $\ln[\sinh(\alpha_g \sigma)]$ and the adjustable stress multiplier α_g (MPa^{-1}) is iterated that brings ($\alpha_g \sigma$) into the correct range yielding parallel linear lines (with slope as n_g) for different temperatures.

The power–law and the exponential plots between $\dot{\varepsilon}$ and σ do not reveal the distinct deviation as observed for creep data and hence for hot deformation, they assume the following forms

$$\dot{\varepsilon} = A_p (\sigma)^{n_p} \ e^{-Q/RT} \qquad (2)$$

$$\dot{\varepsilon} = A_e \ e^{(\beta_e \sigma)} \ e^{-Q/RT} \qquad (3)$$

where n_p, β_e are stress exponents; A_p and A_e are constants. In the above relations, n_p and β_e values obtained at a given strain for hot deformation correspond to those for the entire stress/ strain rate range. If the stress multiplier is determined as $\alpha = \beta_e / n_p$, then this α is designated as α_{ER} (i.e., $\alpha_{ER} = \beta_e/n_p$), where the subscript 'ER' indicates that it is determined by fitting the power and the exponential laws for the entire strain rate range. Whereas, those determined by force fitting the Garofalo equation (1) are designated as α_g and n_g.

An important question that is addressed is whether any relationship exists between the two stress multipliers, viz. α_g and α_{ER}. This is useful, because evaluating the adjustable α_g by the iteration method involves much of the computational time. And for a given material, once the relationship between α_g and α_{ER} is established for the investigated strain rate–temperature domain, α_g can be evaluated by knowing α_{ER} which is much easier to get. A new relationship is proposed between α_g and α_{ER} in terms of n_p for the data obtained from hot compression tests on modified 9Cr–1Mo (P91) steel over a wide range of strain rate (0.001–100 s^{-1}) and temperature (1123–1373 K). Using the α_g values calculated following the proposed relationship; the other constitutive parameters n_g, Q and $\ln A_g$ were determined at various strains. On incorporating the strain dependence of these parameters, prediction of flow curves was performed following the Garofalo equation (1). The predicted flow curves are compared with those experimentally obtained over the entire investigated strain rate–temperature domain.
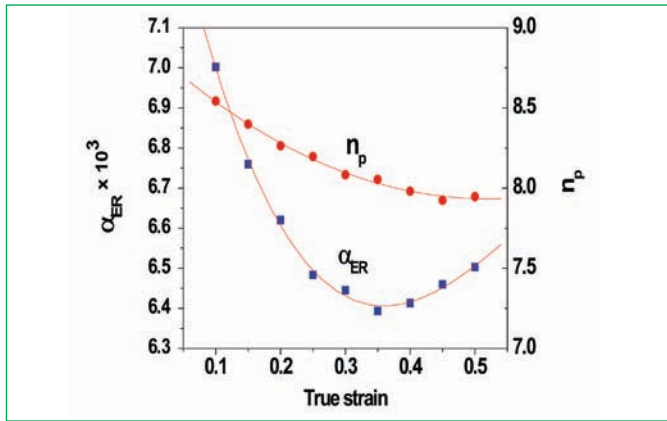
Figure 1: Variation of average values of α_{ER} and n_p with true strain

Figure 2: Linear dependence between (α_g/β_e) and n_p at strain = 0.15 (R=0.96)

The flow stress data at different strains (0.1–0.5 at steps of 0.05) were analyzed to determine α_{ER}. Towards this, n_p and β_e were evaluated at different strains and the values of n_p and β_e were determined as reciprocal of slopes of lines in the plots ln (σ) vs. ln($\dot{\varepsilon}$) and σ vs. ln($\dot{\varepsilon}$), respectively at different temperatures. For calculating α_{ER}, the respective values of n_p and β_e obtained at different temperatures (1123–1373 K, at intervals of 50 K) were used and α_{ER} at each temperature was obtained as $\alpha_{ER}= \beta_e/n_p$ thus giving the average value of α_{ER} at respective strains. The strain dependence of the average values of n_p and α_{ER} is shown in Figure 1.

The important observations that led to the formulation of the relationship between α_g and α_{ER} are presented for strain = 0.15 as an example. Though the average value of n_p = 8.398 at strain = 0.15 (Figure 1), it was noticed that n_p was found to decrease from 11.058 to 6.388 with increasing temperature

from 1123 to 1373 K. The analysis also revealed that the same trend was observed for the variation of (α_g/β_e) with temperature, i.e., (α_g/β_e) was found to decrease from 0.1973 to 0.1397 with increase in temperature from 1123 to 1373 K; α_g=0.00886 MPa^{-1} at strain of 0.15. This suggested that (α_g/β_e) would increase with increase in n_p and such a plot is shown in Figure 2, typically for strain of 0.15 which reveals that (α_g/β_e) $\propto$ n_p. Similar behavior was noticed at all strains for the strain range 0.1–0.5 at steps of 0.05. From the definition of $\alpha_{ER}=\beta_e/n_p$, it follows that

$$(\alpha_g/\beta_e)= [\alpha_g/(\alpha_{ER}\times n_p)] \propto n_p.$$

Therefore, (α_g/α_{ER}) would show a linear dependence with $(n_p)^2$. The (α_g/α_{ER}) was calculated at various strains (0.1–0.5, steps of 0.05) for different temperatures (1123–1373 K, 50 K interval). The plot of (α_g/α_{ER}) vs. $(n_p)^2$ is shown in Figure 3 which clearly demonstrates that the data could be described by linear relationship. Hence, the new relationship
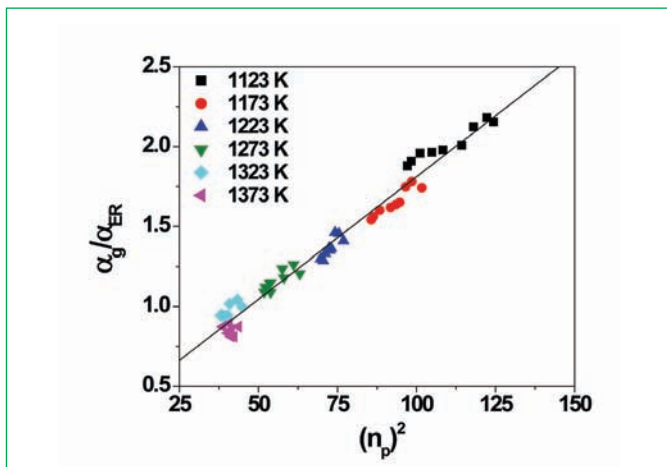

Figure 3: Proposed relationship between α_g and α_{ER} in terms of n_p for the strain range (0.1–0.5 at intervals of 0.05) for P91 steel (R=0.988)
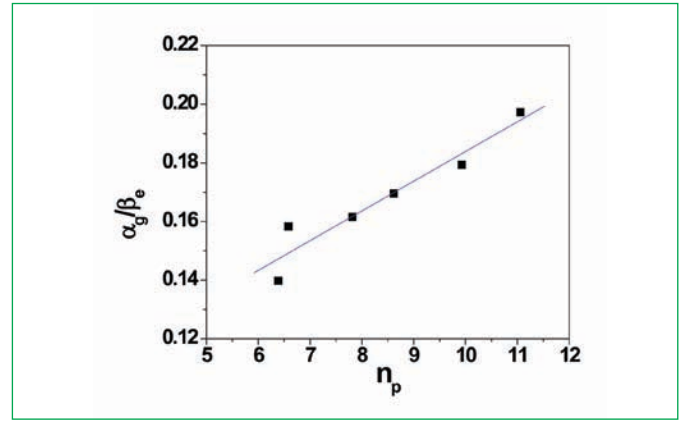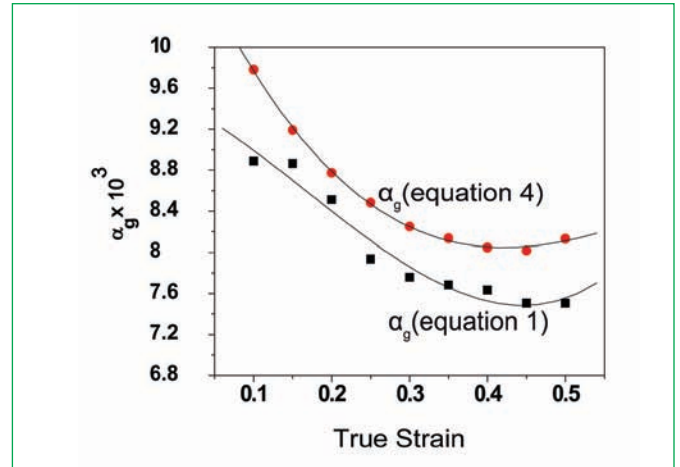

Figure 4: Variation of α_g with true strain. The α_g values obtained by iteration method after Equation (1) are also shown along with the polynomial fits
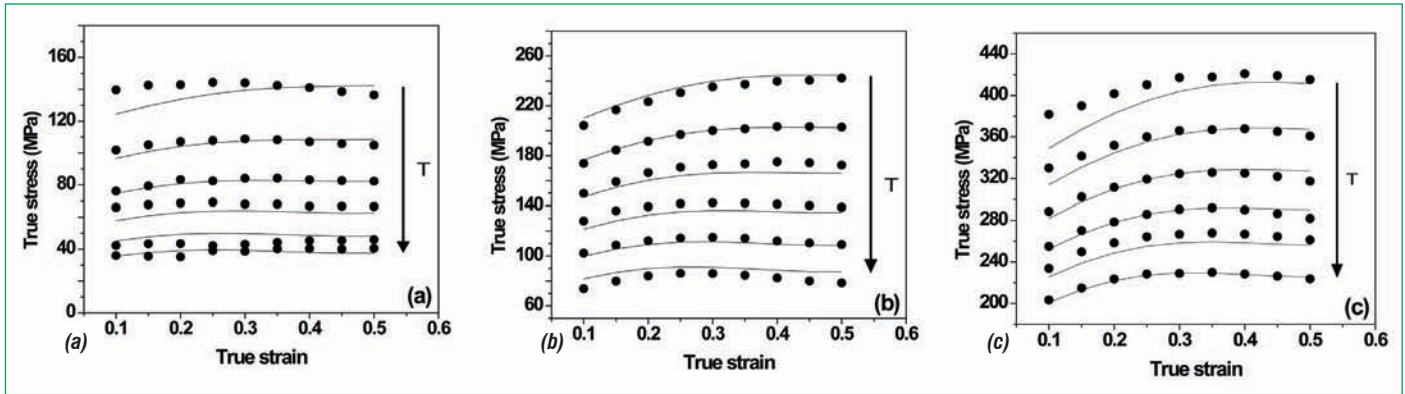
Figure 5: Typical predicted(—) flow curves and their comparison with those experimentally(●) obtained at strain rates of (a) 0.001 s⁻¹, (b) 0.1 s⁻¹ and (c) 100 s⁻¹ in the temperature range 1123–1373 K at intervals of 50 K

between the stress multipliers α_g and α_{ER} for the modified 9Cr–1Mo (P91) steel can be proposed as

$$\frac{\alpha_g^\varepsilon}{\alpha_{ER}^\varepsilon} = 0.27977 + 0.01531\left(n_p^\varepsilon\right)^2 \qquad (4)$$

where the superscript ε indicates the strain dependence. An important implication of the above proposed relationship (equation 4) is that knowing α_{ER} and n_p at each strain, α_g values can be easily determined. Figure 4 shows the variation of α_g with strain and for the sake of comparison, the adjustable α_g values based on the iteration method obtained by force fitting equation (1) are also shown in this plot. After calculating α_g, following the Garofalo equation (1), the other constitutive parameters such as n_g, Q and $\ln A_g$ were evaluated. While n_g was found to be independent of true strain (n_g = 5.0369), Q and $\ln A_g$ varied with strain. It was observed that Q was in the range 368.7–395.9 kJ/mol and $\ln A_g$ was in the

range 30.7–33.7. Further, the strain dependences of α_g, Q and $\ln A_g$ were best described by 3rd order polynomial fits and were used for prediction of flow stress following Garofalo equation (1).

Prediction of flow stresses was performed for the investigated strain rate (0.001–100 s⁻¹) and temperature range (1123–1373 K at intervals of 50 K) according to the equation given below which is obtained by rearranging equation (1) as

$$\sigma = \frac{1}{\alpha_g}\left(\sinh^{-1}\left(\frac{Z}{A_g}\right)^{\frac{1}{n_g}} \right) \qquad (5)$$

where Z is the well known Zener–Hollomon parameter and $Z = \dot{\varepsilon}\, e^{(Q/RT)}$. The typical predicted flow curves and their comparison with those experimentally obtained are shown in Figures 5 (a)–(c) for the data at lower (0.001 s⁻¹), intermediate (0.1 s⁻¹) and higher (100 s⁻¹) strain rates at various temperatures. It could be observed that the predicted flow stresses are in good agreement with those experientially measured. The analysis of standard statistical parameters determined for the data in entire range of strain, strain rate and temperature (Figure 6) revealed that the correlation coefficient, R = 0.994 and average absolute relative error, AARE = 5.03%. Thus it can be concluded that α_g and in turn the other constitutive parameters (n_g, Q and $\ln A_g$) obtained based on the proposed new relationship between the stress multipliers α_g and α_{ER} (i.e. equation 4) can be successfully employed for predicting the flow behavior of modified 9Cr–1Mo (P91) steel in the investigated strain rate–temperature hot working domain.
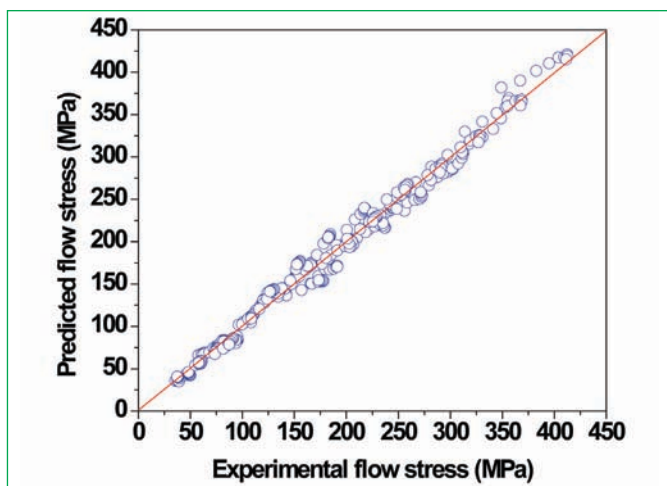

Figure 6: Correlation between the predicted and experimental flow stresses for the strain range 0.1–0.5 (at intervals of 0.05) over the entire strain rate (0.001–100 s⁻¹) and temperature range (1123-1373 K)

*Reported by C. Phaniraj and colleagues,
Materials Technology Division, Metallurgy and Materials Group*

Design Development and Commissioning of Electrical Sub-system of PFBR Operator Training Simulator

One of the key elements that determine the operational safety of any nuclear power plant is the technical knowledge of its operators about the behaviour of the plant. To ensure safety in the operation of any nuclear power plant, comprehensive training of its operators in all phases of the plant operation is essential. Essentially teaching and training are the cornerstones of the efficiency of the operators. The operators need to understand the plant dynamics and acquire the capacity to react effectively when facing unusual situations. Technical knowledge can be imparted by classroom training and on-line training. However online training for all operating and emergency conditions is practically impossible from safety considerations of nuclear power plant. A viable alternative to online training is the use of training simulators. It is widely recognized that training simulators play an essential and extremely important role in establishing viable training programmes for operators of nuclear power plant. Simulators are designed to replicate the plant condition under various operating and emergency conditions. Computer simulation represents the application of mathematical models of real systems to derive its characteristics and behaviour without actually constructing or operating the system.

As per the guidelines of Atomic Energy Regulatory Board, nuclear power plant operators need to be trained and certified in Full Scope Replica Simulator before being given license to operate nuclear power plant. In order to meet this requirement, a Full Scope Replica Simulator for PFBR was designed and developed by Computer Division in collaboration with the then Reactor Engineering Group and Nuclear & Safety Engineering Group. The most important sub-systems of the training simulator are neutronics, primary sodium, secondary sodium, steam water and electrical system. The design, development and commissioning of the electrical sub-system of the simulator was carried out by Computer Division in collaboration with PPCD/REG.

Electrical power system is the source of power for the reactor coolant pumps and other auxiliaries during normal operations and for the protection system and engineered safety systems during normal and accident conditions. Hence it has to be interfaced with all the other sub-systems. The electrical system consists of class IV normal AC power supply, class III emergency AC power supply, class II AC instrumentation and control power supply, class I DC instrumentation and control power supply as depicted in Figure 1.

Class IV power supply system receives the power from the grid as well as from the turbo-generator. It feeds the class IV 6.6 kV and 415 V loads and the class III power supply system. The class III power supply system receives the power from the class IV system and the diesel generator. It feeds the class III 6.6 kV and 415 V loads and class II and class I system. The class II power supply system receives the power from
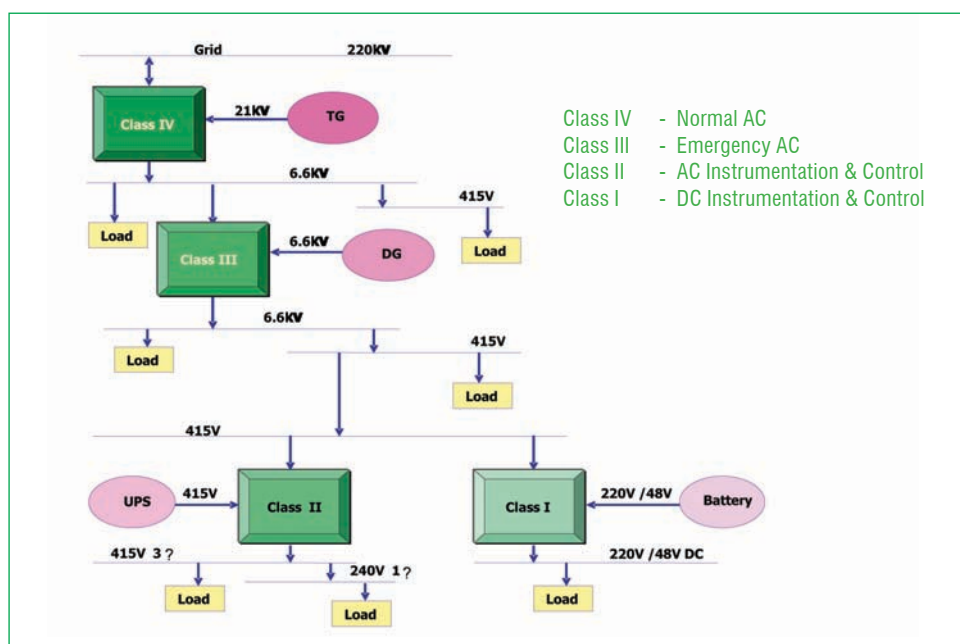

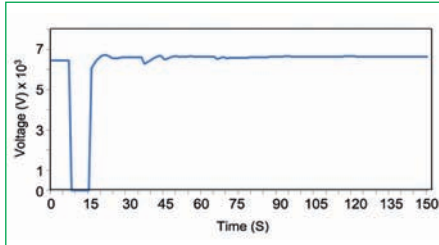Figure 1: Schematics of the PFBR electrical system

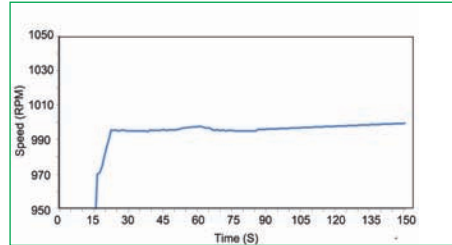Figure 2: Class IV power failure-emergency bus voltage

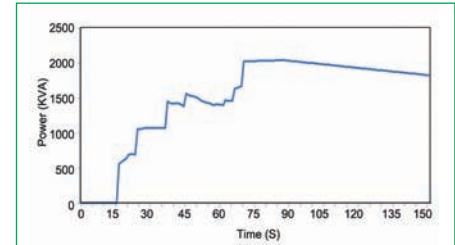Figure 3: Class IV power failure-diesel generator speed

Figure 4: Class IV power failure-diesel generator power

class III 415 V system and 240 V UPS system. It feeds the 415 V three phase and 240 V single phase loads. Class I power supply system receives the power from class III 415 V system and from 220 V / 48 V batteries. It feeds the 220 V / 48 V DC loads.

The development includes process modelling, logic modelling and virtual panel modelling. Process model represents the network functioning of the electrical system. The logical model represents interlocks and controls of various equipments. The virtual panel model represents control panel and console panel in soft form. The interfaces between the process, logic and virtual panel models are established by passing the necessary signals. Design data pertaining to various equipments like turbo generator, generator transformer, unit auxiliary transformer, station transformer, transmission lines, bus coupler, circuit braker and loads etc. were collected from the designers and modelled. The electrical network was created, compiled and tested. The control schematic of the electrical network was modelled through logic modelling. Virtual panels are screen-based soft-panels, which emulate control panels with animated panel equipment icons. During the development stage of the simulator, virtual panels are designed and created. It is used for testing and debugging the simulator during various stages of development and maintenance. All the modelling has been completed. The electrical system was also integrated with other simulator sub-systems. The integrated system was tested for normal operation and various transients. The integrated system was ported to the simulator hardware at BHAVINI and integrated with the hardware panels. This system

with the hardware panels was tested for continuous normal operation and various transients. The system has been demonstrated to the internal and external verification and validation committee and the clearance has been obtained. In addition to the normal operation, the transients demonstrated are generator trip resulting in power setback, offsite power failure resulting in turbo-generator operating with 'house load', class IV power failure with diesel generator feeding the emergency loads as per the emergency transfer scheme, station blackout resulting in class II and class I loads fed by UPS and battery bank respectively, transfer of unit auxiliary transformer loads to station transformer under fault conditions in either unit auxiliary transformer or generator transformer, transfer of station transformer loads to unit auxiliary transformer under fault conditions of station transformer and system getting isolated from the grid, due to grid disturbance. Normal operation and all the above transients are cleared by the verification & validation committees. One of the transients namely class IV power failure with DG feeding the emergency loads as per the emergency transfer scheme is explained below.

The failure of class IV power supply can occur due to the simultaneous power failure from the grid and turbo-generator. Due to the class IV failure all the loads connected to class IV and class III buses will trip. All the diesel generators will start on sensing the power failure in the class III buses after a pre-determined delay. Diesel generator voltage and frequency will pick up and diesel generator incomer circuit breaker will close. When the incomer closes, class II and class I system loads will be fed by diesel generator power supply. The class III loads will be restored according to priority specified in the emergency transfer scheme.

Figure 5: Class IV power failure—primary sodium pump (PSP) speed and pony motor speed

The electrical parameters like emergency bus voltage, diesel generator speed and power primary sodium pump speed and pony motor speed are recorded and the corresponding profiles with respect to time, obtained during the testing of the simulator, are shown in Figures 2, 3, 4 and 5 respectively.
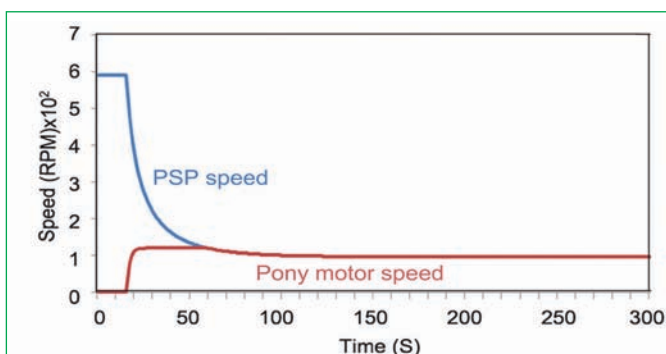
Reported by K.K.Kuriakose and colleagues,
Computer Division, EIRSG

Young Officer's FORUM

Shri Govind Kumar Mishra received his B. Tech Degree (Electronics & Instrumentation Engineering) in 2007 from Uttar Pradesh Technical University, Lucknow and M. Tech Degree in Nuclear Science & Engineering in 2011 from Homi Bhabha National Institute, Mumbai. He is from the 2nd batch of BARC training school at IGCAR campus and currently working as Scientific Officer in Process Instrumentation Section, ICD/PPG/RDG. His current area of interest is in the field of process instrumentation control, design and development for FBRs.

Indigenous Data Acquisition and Processing System for Integrated Top Shield Test Facility

In Prototype Fast Breeder Reactor (PFBR), top shield consists of roof slabs, large rotatable plug, small rotatable plug and control plug. It receives heat from hot pool sodium and loses heat by

(i) partial removal through internal cooling system

(ii) heat removal by vault cooling system after complex heat exchange, through main vessel, safety vessel and its insulation, reactor vault liner and

(iii) heat loss from its top surface. Maintaining the temperature and temperature difference across the top shield is important to limit the thermal bowing of the top shield.

Thus, thermal design of top shield is a complex process, which needs detailed theoretical and experimental investigation and verification. Towards this an experimental test facility, Integrated top shield test facility (ITSTF), has been conceived, constructed and commissioned (Figure 1) at IGCAR.

This is a practical working model of top shield of PFBR, which includes hardware, software, blowers and associated piping and components. Currently it is used for studying the cellular convection, thermal heat flux and temperature difference across

the top shield. This facility, being an exact replica of PFBR top shield, can be utilized for training and demonstration purpose for PFBR personnel.

Integrated top shield test facility

ITSTF is provided with the following instruments and electronics to collect the temperature reading from 900 thermocouples (approx.) simultaneously.

- Thermocouple (Approx 900 nos. on different locations)
- Unimux-pro (universal input module) and Moxa N-port (media converter) based data acquisition system
- MW-100 with universal input module based data acquisition system
- Panel for housing the electronics with terminal block and power supply arrangement
- Local area network for communication within facility
- Local control room for temperature monitoring and heater control
- Main control room for records and display
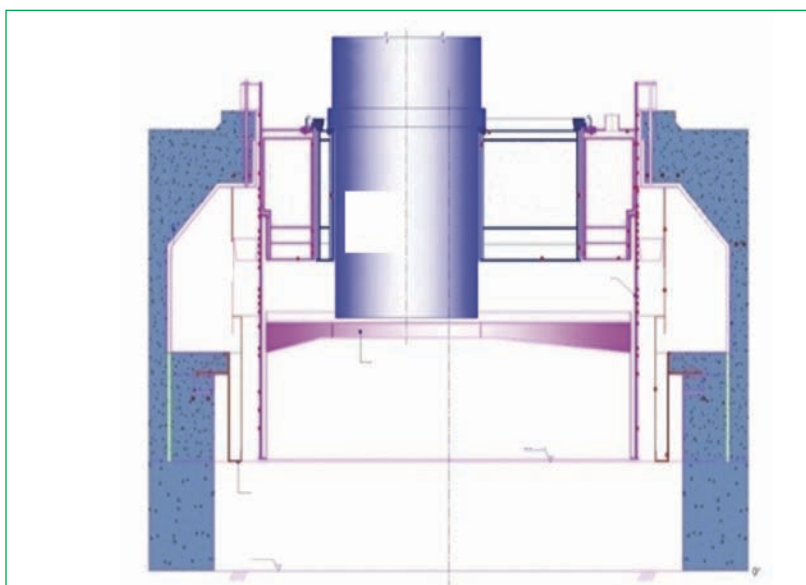- Heaters with PID controller.

Figure 1: Integrated top shield test facility along with typical location of thermocouples
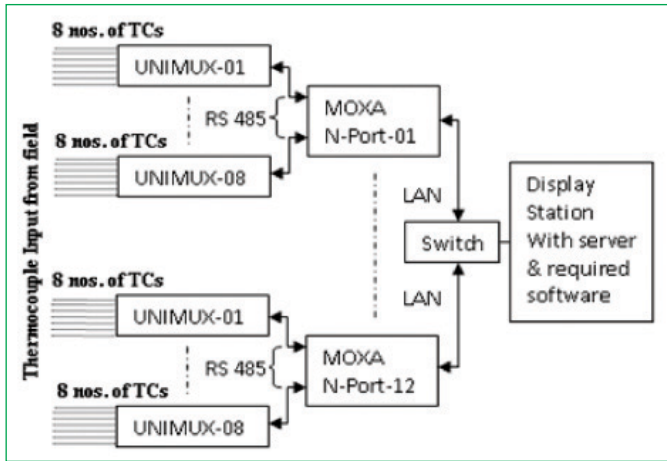
Figure 2: Connection details of UNIMUX based temperature data acquisition software

Table-1: Location and quantity of thermocouples

S. No.	Location/component	Quantity
1.	Main vessel shell and roof slab outer shell	172
2.	Reactor vault	60
3.	Roof slab heater plate (top surface + bottom surface + inner surface)	84 (48+12+24)
4.	Roof slab	88
5.	Small rotatable plug	74
6.	Cylindrical shell	120
7.	Control plug	300
	Total	898

Thermocouple and their locations

Thermocouples 2 mm Φ, type K are provided at different locations, elevations and angles to monitor the temperature of ITSTF. Electronics are housed in the panels for connecting and processing the thermocouple input signals. Thermocouple signals are extended to the electronics located inside the panel mounted on the facility as well as kept inside the local control room. Locations and quantity of thermocouples are given in Table 1.

Challenges

i) Robustness in design and construction, installation of thermocouples in complicated locations and routing them up to accessible locations

ii) To have I&C system, which works in air conditioning as well as harsh environment

iii) Transmitting the signals to a long distance from the site to control room

iv) Development of mimics and associated software to process and display results to understand the physics of heat transfer for process at various regions, cellular convection, radiations and conduction

v) User friendly design and cost effective

Temperature data acquisition system

Two types of temperature data acquisition systems are provided to measure the temperature of ITSTF.

i) Unimux-pro (universal input module) and Moxa N-port (media converter) based data acquisition system.

ii) MW-100 with universal input module based data acquisition system.

First set of data acquisition system consists of Unimux-pro (universal input module), configured for 'K' type thermocouple input, Moxa N-port (media converter) and LAN switch. The

Unimux module has eight input channels. The acquired signals from the thermocouple is digitized and sent to Moxa N-port media converter. This is receiving data as RS-485 signal, converts it to TCP/IP and having its IP number for easy access and control using LAN. In this arrangement 8 Unimux are connected in daisy chain with Moxa N port module. All the thermocouple signals connected to Unimux are monitored at display station in control room through LAN connection (Figure 2). Temperature can be monitored locally also with the help of PC or Laptop.

Available software at display station in control room

- Unitool: Hardware specific software for configuration and communication check
- Labview 8.2 with Lab VIEW Data logging and supervisory control module
- Cataserver Exe.OPC server
- Lab view OPC server

Software development for monitoring and configuring the thermocouple signals

The data acquisition software has been developed to read the temperature data using labview 8.2 version for above set of hardware. In this software dedicated OPC server (cataserver opc) will communicate with Moxa N-port ethernet gateway controller and NI OPC client simultaneously using data socket to receive the temperature data for monitoring and recording.

OPC Client/Server technology

OPC is a widely accepted industrial communication standard that enables the exchange data between multi-vendor devices and control applications without any proprietary restrictions. An OPC server can communicate data continuously among third party devices or PLC on the shop floors, RTU in the field, HMI stations and software applications on desktop PCs. Even when the hardware and software are from different vendors, OPC compliance makes continuous real time communication possible.
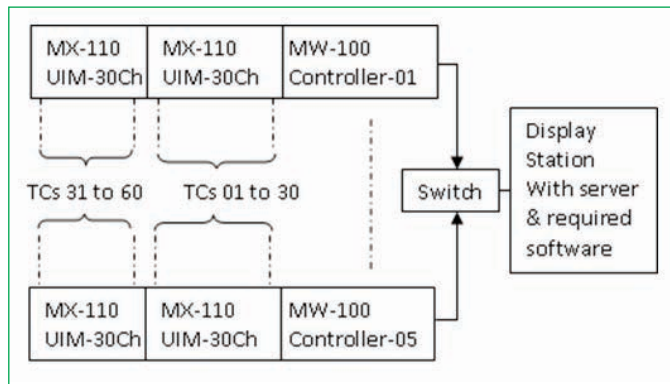
Interoperability is assured through the creation and maintenance of non proprietary open standard specifications.

Data Socket overview

Data socket is an internet programming technology based on TCP/IP that simplifies data exchange between computers and applications. Previously there were different types of hardware, software and protocols involved in various applications. This complexity forced a programmer to negotiate between the different protocols to transfer data, which requires a great amount of development time and resources. As a solution to this, National Instruments developed a data socket method of programming which eliminates the complexities of hardware and software integration specifically in test and measurement applications. It was also developed specifically for publishing and sharing the live data over many different protocols (DSTP, OCP, HTTP, FTP and local file access). In addition to providing an overlapping interface for many protocols, it also transfers data in a self describing format that can include string, scalars, booleans and waveforms.

Problems faced in this arrangement

- Malfunctioning of unimux (input module)
- Frequent loss of communication
- Poor stability

To solve the above problems

- Faulty/malfunctioning Unimux input modules were replaced with available spare modules (same type)
- Unitool software was reinstalled and all the input modules were reconfigured
- Stable values were considered for the experiment

Second set of data acquisition system consists of MX110-UNV, 30 channels universal input module configured for 'K' type thermocouple input, MW-100 controller used for accessing the temperature data from input modules and converting it suitable for TCP/IP communication and LAN switch. All the thermocouple signals connected to MW-100 main unit are displayed in the display station located in control room using LAN connection.

Available software at display station in control room:

- Gate MW interface software: used for integrating the multiple units of MW-100 in a single project.
- DAQ logger software for monitoring and recording the temperature data.
- Add observer software for developing the mimic diagrams.

Software development for monitoring and configuring the thermocouple signals

The data acquisition software has been developed to read the temperature data using Gate MW interface software and DAQ logger software for above set of hardware. In this software dedicated Gate MW interface software will communicate with MW-100 controller and DAQ logger software simultaneously using TCP/IP to collect the temperature data for monitoring and recording (Figure 3).

The temperature data acquisition software developed currently is to acquire 300 thermocouple input signals from the test facility. All the five MW-100 data acquisition systems (60 channels each) are configured and connected to computer through gate MW interface software for monitoring and recording all the channels simultaneously at one place. DAQ logger software is utilized for scanning and recording the real time data in the form of groups assigned based on the location of the thermocouples in the test facility.

Mimic development

Dedicated mimic diagrams have been developed for displaying the data in the display station. Mimics are developed using ADD observer software builder and same mimic can be operated using ADD observer software panel for accessing the real time temperature data online.

Temperature data acquisition system for ITSTF was successfully commissioned for monitoring and recording the temperature of 900 thermocouples (approx.) simultaneously at single location. Graphical user interface software for easy and effective monitoring was developed for both types of data acquisition systems.

Presently heat/temperature at the bottom of top shield is getting generated by the use of electric heater of appropriate rating. In future it is planned to have the facility filled with sodium capacity at the bottom of top shield and exact heat flux should be generated by the same, to understand the exact behavior of the top shield and its components under sodium environment. I&C system needs to withstand the sodium environment conditions.

Reported by
Govind Kumar Mishra, Power Plant Group,
Reactor Design Group

Young Researcher's FORUM

Structural, Vibrational, Dielectric and Magnetic Properties of Multiferroic La-substituted BiFeO$_3$-PbTiO$_3$

Mr. Karuna Kara Mishra did his Master in Physics from Sambalpur University, Sambalpur, Odisha. He joined Light Scattering studies section, CMPD, MSG, IGCAR as a DAE research fellow in August 2007. He has submitted his doctoral thesis titled "Raman and Brillouin spectroscopic studies of Phase Transitions in Perovskite Ferroelectric Materials" in 2012 to Homi Bhabha National Institute, Mumbai under the guidance of Dr. A. K. Arora.

Multifunctional materials that couple electric, magnetic, and structural order parameters resulting in coexistence of ferroelectric, ferromagnetic and ferroelastic behaviors have attracted considerable attention in recent years. There is a growing interest in complex ABO$_3$ type Perovskite multiferroics, which exhibit magnetoelectric effect. Such materials find applications in areas such as transducers, magnetic/ferroelectric data storage, spintronics and magnetic sensors. In this context, rhombohedral BiFeO$_3$ (BF) is unique among other multiferroic materials due to the coexistence of two types of long-range order: antiferromagnetic order below the Neel temperature T_N = 643 K and the ferroelectric order below Curie temperature T_C = 1100 K. However, the compound was not found to show the magnetoelectric effect, as the spiral modulated spin structure led to disappearance of overall magnetization. In addition, the electric polarization was also found to be quite low. Furthermore, the synthesis of ideal Perovskite phase of pure BF is difficult because of comparable thermodynamic stability of Fe^{3+} and Fe^{2+} states of iron in this compound. In order to improve the multiferroic performance of BF and to obtain a stable Perovskite phase different kinds of chemical substitutions have been tried. Recently, It was pointed out that the mixed crystals of BiFeO$_3$-PbTiO$_3$ (BF-PT) with ratio around 50:50 favor the formation of chemically ordered micro-regions in which spiral spin modulation decreases. It has been argued that the incorporation of La^{3+} at A site of BF-PT leads to destruction of spiral modulated spin structure. A few investigations on magnetic and polarization behaviors of La-modified BiFeO$_3$-PbTiO$_3$ with different ratio of BF and PT have been reported. However, there is no study on the effect of La on the evolution of magnetic and polarization behaviors of 0.50(Bi$_{1-x}$La$_x$FeO$_3$)-0.50(PbTiO$_3$) (BLFPT$_x$) in the full range of x.

In this article the results of a detailed study of BLFPT$_x$ using several techniques are presented. Samples were synthesized using solid state reaction method. Structure at ambient and at elevated temperature was investigated using X-rays diffraction. The vibrational spectrum was studied using Raman spectroscopy. Raman spectra were analyzed quantitatively to obtain mode frequencies, their line-width and intensities. The dielectric behaviour and the polarization were probed to confirm the relaxor nature of the sample. The magnetization measurements were made in field-cooled and zero field-cooled conditions to understand the nature of magnetic ordering in the system.

Polycrystalline BLFPT$_x$ powder samples were synthesized for x = 0.0, 0.2, 0.3, 0.4 and 0.5 by the solid-state reaction technique. The calcined powders were pressed into pellets and sintered. X-ray powder diffraction patterns of the sintered samples were measured to determine the structure and confirm the phase purity. Energy Dispersive X-ray spectroscopic (EDS) measurements were carried out on pellets of all the samples to study the chemical composition. The EDS spectrum shows the presence of all the cationic elements (Figure 1). The compositions (final stoichiometry) estimated from EDS spectra were found to be in fair agreement with those of the starting compositions. The scanning electron micrograph (inset(a)) taken on fractured surface of pellet show uniform distribution of grains. The grain size is slightly different for each La-content, but there is no correlation between the two parameters. The density of all samples was between 96.5 and 99% of the theoretical density. The selected area electron diffraction pattern (inset(b)) indicate the polycrystalline nature of all samples and are indexed to the tetragonal phase for $0 \le x \le 0.3$ and to cubic for $x \ge 0.4$.

Structural properties

Figure 2(a) shows X-ray diffraction patterns of the pure and La-substituted BF-PT ($0 \le x \le 0.5$). All the diffraction peaks could be indexed to the tetragonal phase with space group $P4mm$ for $x \le 0.3$. The tick pattern shown at the bottom of the figure is the calculated peak positions for the tetragonal phase for x = 0. From the X-ray reflections, it can be seen that as there are no unindexed lines, the compounds are single phase. The (001) reflection at 20° 2θ is found to shift towards (100) peak and the two merge at x = 0.4. This suggests a reduction in the c-cell parameter of tetragonal phase as x increases and attaining a value same as that of cell parameter a for x = 0.4. Similar merging of doublets at 2θ ~ 32°, 47° and 53° is also found corresponding to (101)-(110), (002)-(200) and (201)-(210) reflections, respectively. One can notice from Figure 2(b) that the lattice anisotropy (c/a) becomes smaller with increasing La-content. For $x \ge 0.4$, the diffraction patterns fit to a cubic structure with space group $Pm3m$. Thus,
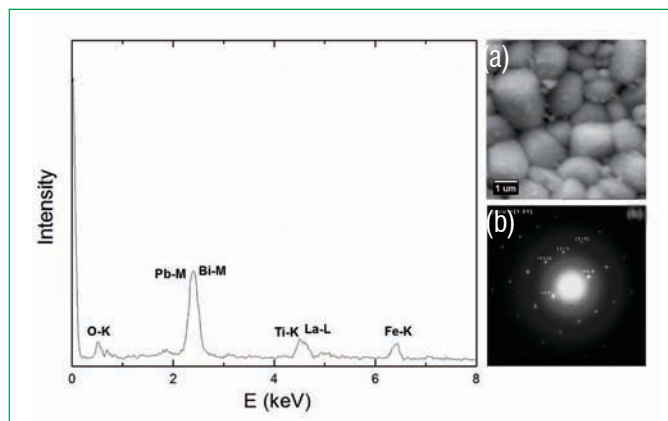
Figure 1: EDS spectra of BLFPTx for x = 0.4. Inset (a) shows the SEM image and inset (b) shows SAED pattern

Figure 2: (a) X-rays diffraction patterns of BLFPT$_x$ ($0 \leq x \leq 0.5$) and (b) Variation of c/a ratio for BLFPT$_x$. Inset shows the ABO_3 Perovskite structure displaying BO_6 octahedron

the structural change from tetragonal to cubic phase arises due to the homovalent substitution of Bi (ionic radius 1.34 Å) by La (ionic radius 1.36 Å). An unusually large tetragonality ($c/a = 1.133$) is found for $x = 0.0$, which decreases to 1.022 for $x = 0.3$. For $x = 0.4$, the tetragonal distortion disappears and a cubic phase with lattice parameter $a = 3.9467(2)$ Å emerges. *In-situ* X-ray diffraction measurements at high-temperature were carried out to study the structural stability of tetragonal BLF-PT solid-solution for $x = 0.0$, 0.2 and 0.3. The X-ray diffraction patterns as a function of temperature were obtained using an Edmund Buhler high temperature attachment. The X-ray diffraction patterns were analyzed to obtain the unit cell parameters. Figure 3 shows a- and c-cell parameters as a function of temperature for $x = 0$ sample. One can see that the sample exhibits an unusually large anisotropy, which decreases with the increase in temperature from $c/a = 1.133$ at ambient to 1.0 at 988 K. At this temperature the tetragonal distortion disappears and a cubic unit cell with $a = 3.9875(9)$ Å is found. The lattice parameters for $x = 0.2$ and 0.3 show similar behavior as $x = 0$ sample with temperature and the tetragonal-cubic transition is found to occur at 773 and 618 K, respectively. This data was used to construct a x-T phase diagram. One can see in Figure 4 that at higher x the transition occurs at lower temperatures. From these results it emerges that the anisotropy of the La-substituted BF-PT system depends both on the composition and the temperature. Increasing x as well as
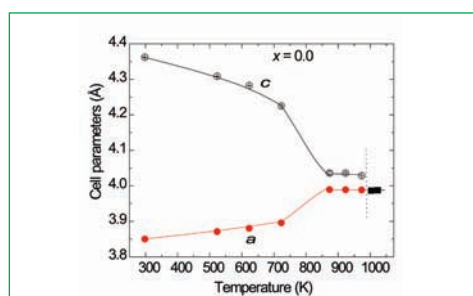
T reduces the anisotropy and the system transforms to a cubic phase. Thus, the decrease in the anisotropy of BLFPT$_x$ upon La-doping is essentially responsible for the lowering of T_c.

Vibrational spectra

In order to understand the nature of the phonons in this mixed-crystal system and to probe the crystallographic phase transition, Raman spectra were measured on all the ($0.2 \leq x \leq 0.5$) samples at ambient and is shown in Figure 5. The irreducible representation of optical phonons in the tetragonal phase *P4mm* is $\Gamma_{opt} = 3A_1 + 4E + B_1$, where A_1 and E modes are both Raman and Infrared active, whereas the B_1 mode is only Raman active. However, the irreducible representation for the optical phonons in the cubic phase (*Pm3m*) is $\Gamma_{opt} = 3F_{1u} + F_{2u}$, where the F_{1u} mode is infrared active and F_{2u} is a "silent mode", since it is inactive both in the Raman and in the infrared. Thus, no Raman active modes are expected in the cubic phase. On the other hand, seven of the modes of the tetragonal phase for $x = 0.3$ could be identified unambiguously in the cubic phase also. The modes in the cubic phase that have correspondence with those of the tetragonal structure appear to arise due to the breakdown of the Raman selection rule due to the substitutional disorder at the cation site and essentially represent the phonon density of states. In order to examine the manner in which total Raman intensity depends on the composition, we measured the Raman spectra

Figure 3: Variation of the c and a lattice parameters as a function of temperature for x = 0

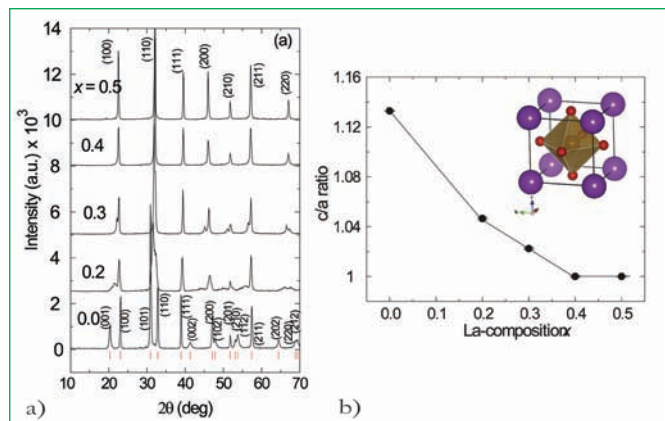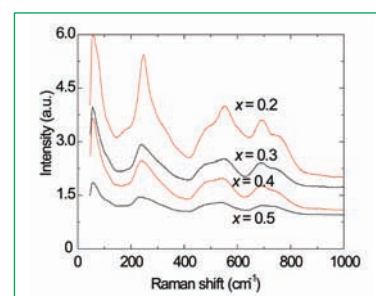Figure 4: x-T phase diagram of the tetragonal BLFPTx solid-solution

Figure 5: Raman spectra of BLFPTx samples at ambient

at large number of spots on each pellet and obtained the average integrated intensity (integrated from 40 to 1000 cm^{-1}). In order to make this intensity free from extrinsic factors such as laser power, focusing and alignment, the intensity of a fused-quartz plate, placed next to the pellet, was also measured as a reference sample. Raman intensity from quartz plate was also integrated in the same spectral range. The total Raman intensity is shown in Figure 6 after normalizing with that of the quartz. One can see that the scattered intensity decreases rapidly as x approaches tetragonal-cubic transition boundary. As the tetragonal distortion (c/a - 1) is only 0.022 at x = 0.3, the Raman intensity has exhibited a large decrease as compared to lower x values. The fact that intensity does not become zero in the cubic phase implies that the symmetry-forbidden scattering is significant. In other words, the presence of polar nano-regions (PNRs) in cubic phase could contribute to the Raman scattering process.

Raman spectra of pure and La-substituted BF-PT samples at elevated temperature starting from 298 to 873 K were also measured (Figure 7). At elevated temperature the spectra broaden further and the intensities are found to reduce. These spectra were analyzed using Lorenzian fitting to obtain the spectral parameters and investigate its behaviours with temperature. An analysis of parameters such as Raman mode frequencies and the line-widths were obtained to identify the phase transition. The temperature dependence of the line-widths of pair of modes at 488 and 551 cm^{-1} is shown in Figure 8 for x = 0.3. The line-widths of these modes show anomaly around 618 K, associated with the tetragonal-cubic phase transition. These modes are associated with the oxygen vibrations of BO_6 octahedra. As temperature is increased, the anisotropy of the octahedra reduces. As a result, the distribution of B-O bond length is expected to reduce. This can reduce the inhomogeneous broadening of the octahedral vibrations. It may be pointed out that the homogeneous (intrinsic) broadening of phonons in pure compounds is much smaller at ambient and even at elevated temperature as compared to the inhomogeneous broadening in mixed crystals due to bond-length distribution. For example, in pure $BiFeO_3$ the two Fe-O distances are 1.958 and 2.110 Å while in pure $PbTiO_3$ the two Ti-O distances

are 1.97 and 2.032 Å. Thus, in the x = 0.3 sample the B-O bond lengths in BO_6 octahedra are expected to have a range of values. At ambient the average B-O bond length in the x = 0.3 sample in the a-b plane is 1.966 Å while along the c-direction, it is 2.01Å. In the cubic phase the BO_6 octahedron becomes regular with a bond length of 1.983 Å. A regular octahedron is expected to have a narrow distribution of bond lengths. However, this kind of anomaly at T_c for x = 0.0 and 0.2 sample is not found. For x = 0, the T_c is beyond the temperature range covered in the present experiments whereas for x = 0.2, the intensities of the modes discussed above are weak and disappeared before the transition temperature.

Dielectric behaviour

Figure 9 shows real part of dielectric constant (ε_r) as a function of temperature at different frequencies for x = 0.5. It is evident that a diffuse (relaxor-type) phase transition is exhibited by the x = 0.4 and 0.5 samples confirming the presence of PNRs. It can be pointed out here that PNRs are the characteristic feature of relaxor system. Figure 10(a) shows the ferroelectric hysteresis loop of BLFPT$_x$ at ambient. Well defined hysteresis loops were observed with increasing La-composition. However, the saturation of polarization was not found to occur due to inadequate applied electric field. Note that the slope of the major axis of the hysteresis loop, which is proportional to the dielectric constant, increases rapidly in the tetragonal phase (x ≤ 0.3) suggesting that the dielectric response improves considerably as the anisotropy reduces. However, the remnant polarization remains low. The variation of remnant polarization as a function of composition is shown in Figure 10(b). The remnant polarization increases with x rapidly in the cubic phase.

Magnetic ordering

Magnetization loops (M vs H) were obtained using a vibrating sample magnetometer up to a maximum field of ± 50 kOe at ambient and down to 4 K. The M-H curves for all compositions show a hysteresis loop and it does not saturate up to applied field of 6 T. From the hysteresis loop, it can be inferred that magnetization arises because of two contribution. One is the
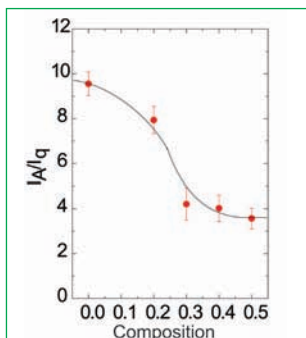

Figure 6: Dependence of normalized integrated intensity on La-composition

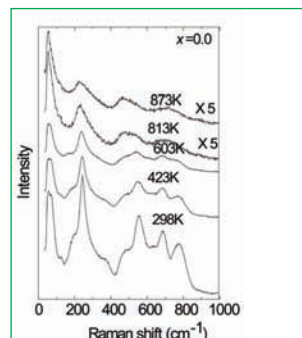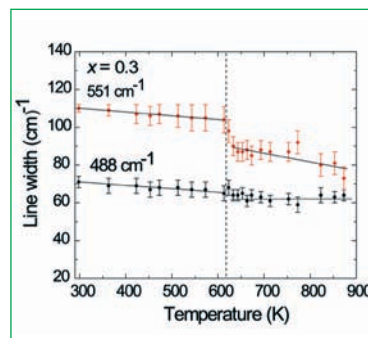Figure 7: Raman spectra of BLFPTx at few selected temperature for x = 0.3

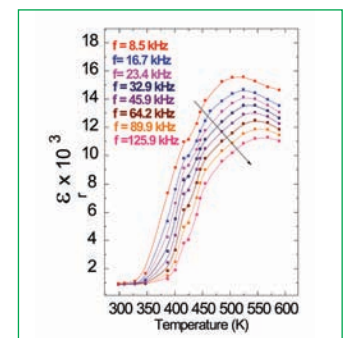Figure 8: Temperature dependence of Raman line-widths for x = 0.3

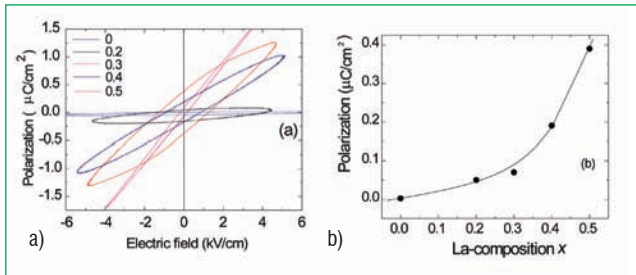Figure 9: Temperature dependence of real part of relative dielectric permittivity at various frequencies

Figure 10: (a) Evolution of polarization (P-E) loop of BLFPTx ($0 \leq x \leq 0.5$) at ambient temperature. (b) Effect of La-composition on the remanent polarization of BLFPTx

Figure 11: a) Magnetic hysteresis loop of BLFPTx for $x = 0.5$ at different temperatures, b) Dependant of FC and ZFC magnetization of BLFPTx at constant static applied magnetic field 1 kOe for $x = 0.2$

ferromagnetic contribution, which gives hysteresis curve and other one arising from paramagnetic host giving rise to a non-saturating linear variation of M at higher field. This suggests the existence of magnetically ordered clusters in an overall paramagnetic host. Formation of magnetically ordered clusters in solid solutions has been reported in other systems also. The remnant magnetization appears to depend on x. This has been argued to be due to the incorporation of La^{3+} in A site of $BLFPT_x$ leading to destruction of spiral modulated spin structure and hence Dzyaloshinskii-Moriya type interaction is enhanced. The M-H loop for $x = 0.5$ at different temperatures is shown in Figure 11a. A hysteresis loop with remnant magnetization appears clearly at 77 K, which becomes more enhanced at 4 K. However, at room temperature all samples are in a paramagnetic state.

In order to understand the nature of magnetic ordering, temperature dependence of magnetization was investigated at applied field of 1 kOe for all the samples. For zero field-cooled (ZFC) magnetization measurement, the sample is cooled from room temperature to 4 K without any external magnetic field and the magnetization is recorded while heating the sample in the applied field of 1 kOe. In case of field-cooled (FC) magnetization, the sample is cooled under the same magnetic field and the magnetization is measured in the heating-run. It was found that the magnetization decreases with temperature and depends on the thermal history of the samples exhibiting irreversibility effect. The temperature at which the ZFC and FC branches coalesce is called irreversibility temperature or magnetic ordering temperature T_{irr}. The T_{irr} is found to shift towards higher temperature with increasing La-composition. The magnetic ordering temperature is related to the average atomic distance of Fe^{+3}-O-Fe^{+3} along a-, b- and c-crystallographic directions. It implies that longer the atomic distance, the lower the ordering temperature. In the case of $BLFPT_x$ system, for $x = 0$, the lattice parameter c of the tetragonal phase is larger than a with largest c/a ratio than other compositions. Hence, the average atomic distance of Fe^{3+}-O-Fe^{3+} along the c-direction is larger than that along a- and b-directions. Therefore, the magnetic interaction along the c-direction weakens earlier than that along a- and b-directions with increasing temperature, making the spin-network break. With
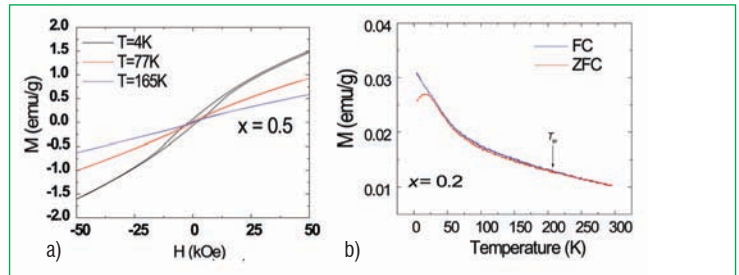
increase in x the c/a ratio decreases and hence the average atomic distance along the c-direction approaches to that along a-direction which in turns enhances the magnetic ordering temperature. Therefore, increase in the magnetic ordering temperature with increasing x is understandable. Furthermore, for $x = 0.2$ sample, the ZFC magnetization shows a cusp at low temperature (Figure 11b). This could be due to a spin glass behavior. In order to confirm this, ZFC magnetization was measured at different static applied magnetic fields and the dependence of the peak temperature on the applied field was obtained. The behavior of magnetic field has been analyzed in the field-temperature plane using Gabay-Toulouse (GT) and de Almeida and Thouless (AT) models. It was found that the data fits well with the AT model ($H^{2/3}$ linear with T_g) implying an Ising spin glass. The exact nature of frozen disorder and magnetic frustration responsible for the spin glass-like behavior is not well understood. However, a possible conjecture is that some of the diamagnetic spin clusters involving Ti^{4+} ion could have embedded into the ferromagnetic matrix involving Fe^{3+} ion because of almost equal ionic radii and short-range ordering of these ions due to charge difference causing the magnetic frustrations and randomness necessary for the origin of spin-glass behavior. The absence of spin-glass behavior for $x \geq 0.3$ implies that La-doping has a significant role in affecting magnetic properties of the systems. However, further studies are needed to explore the role of La in tuning the magnetic properties.

To conclude, pure and La-substituted $Bi_{1-x}La_xFeO_3$-$PbTiO_3$, polycrystalline samples were synthesized. Although no Raman active modes are expected in the cubic phase the presence of several Raman peaks suggests existence of chemically ordered polar nano-regions in the relaxor cubic phase. Increasing x as well as T reduces the anisotropy and the system transforms to a cubic phase. La-doping has a significant role in affecting magnetic properties of the systems. La-substitution in the multiferroic BF-PT system clearly establishes the manner in which the magnetic and dielectric properties are controlled by the tetragonal anisotropy of the system.

Reported by
Karuna Kara Mishra
Condensed Matter Physics Division, Materials Science Group

Conference and Meeting Highlights

11th International Conference on
High Nitrogen Steels and Interstitial Alloys (HNS 2012)
September 27–29, 2012

Shri S. C. Chetal, Prof. M. O. Speidel, Dr. Baldev Raj ,Prof. J.Foct and
Dr. U. Kamachi Mudali during the release of souvenir

The 11th International Conference on High Nitrogen Steels and Interstitial Alloys (HNS 2012) was jointly organized by The Indian Institute of Metals, Kalpakkam Chapter and Ferrous and Metal Sciences Division, IIM with support from Board of Research in Nuclear Sciences, Department of Atomic Energy, Mumbai, at Chennai, India during September 27-29, 2012. HNS 2012 was co-sponsored by Board of Research in Fusion Science & Technology, Gandhinagar, Council of Scientific and Industrial Research, New Delhi, Defence Research & Development Organization, New Delhi, Jindal Stainless Limited, New Delhi, TATA Steel, Jamshedpur, Mishra Dhatu Nigam Limited, Hyderabad, Energietechnik Essen GmbH, Germany and Sandvik, Sweden.

The theme of HNS 2012 was 'High Nitrogen Steels and Interstitial Alloys – Developments and Challenges'. The objective of the conference was to provide a forum to discuss all the developments that have been made in high nitrogen steels and interstitial alloys with a view to identify the new challenges for the future development and applications. The presence of interstitial alloying elements in addition to nitrogen plays a major role in the structure, properties and application of various advanced steels including HNS alloys. The role of such interstitial alloying elements (hydrogen, oxygen, carbon and boron) along with nitrogen also affects the manufacturing, fabrication and application of conventional and advanced austenitic, ferritic, martensitic and duplex steels and stainless steels for a variety of applications in industries. In HNS 2012 these issues were addressed with a focus on automobile, chemical, marine, strategic, power and other important applications.

The conference was inaugurated on September 27, 2012 by Prof. Marcus O. Speidel, senior member of International Scientific Committee on HNS from Swiss Academy of Materials Science, Switzerland. Prof. Marcus O. Speidel explained how nitrogen is gaining importance as an alloying element of stainless steels by making steels more austenitic, stronger, corrosion resistant, wear and fatigue resistant and one day it can replace the costly nickel in toto. Dr. Baldev Raj, President, INAE, President-Research, PSG Institutions and Chairman, HNS 2012 presided over the function. He stressed the importance of addressing the issues concerning the role of interstitial alloys along with nitrogen that affect manufacture, fabrication and application of HNS and developing codes for engineering applications. Prof. Jacques Foct from University de Lille, France, the guest of honor, retraced the beginnings of HNS conference way back in 1988 at Lille, France and reiterated that the growing demand for these conferences confirm the importance of HNS emerging globally and wished the best for HNS 2012. Shri S.C. Chetal, Director, Indira Gandhi Centre for Atomic Research and Co-Chairman, HNS 2012 released the souvenir of HNS 2012 and delivered a key note lecture on "Application of Nitrogen Alloyed Steels for Indian Fast Reactor Programme". Dr. U. Kamachi Mudali, Convener, warmly welcomed the gathering, Dr. M. G. Pujar, Technical secretary, gave a brief overview of HNS 2012 and Dr. Rani P. George, Treasurer, proposed the vote of thanks.

Twenty four technical papers, fourteen invited lectures and two plenary lectures were presented by professionals from reputed academic and research institutions, suppliers, fabricators and user industries during the conference. About

hundred delegates including leading experts from France, Switzerland, Russia, Austria, Germany, Czechoslovakia, Sweden, Poland and India participated in this important event. The delegates were mostly from industries such as steel, power generation, welding consumable, tube, pipe and valve manufacturing, commercial suppliers of steel products, equipment manufacturing, educational institutions, research and development organizations. About seventeen young delegates from academia and R&D put up posters displaying advances in high nitrogen steel research and had interesting interactions with peers and experts. Five best oral

presentations and poster displays selected by eminent judges were presented with prizes.

HNS 2012 provided a platform for international experts and researchers on high nitrogen steels to address recent advances in production of HNS, alloy design, heat treatments, emerging trends in processing and application, surface modification and newer application of HNS. The conference definitely attracted wide participation from industry, research institutions, academia, end user companies and marketing personnel.

Reported by U. Kamachi Mudali, Convener, HNS

Theme Meeting on Structure and Thermodynamics of Emerging Materials (STEM-2012)
November 5-6, 2012

Participants of STEM-2012

The BRNS sponsored theme meeting, 'STEM-2012' focusing on "Challenges and Issues in Surface Modification, Thin Films and Coatings" was organized jointly by Indira Gandhi Centre for Atomic Research and The Indian Institute of Metals – Kalpakkam Chapter during November 5-6, 2012 at Convention Centre, Anupuram. During the inaugural session, Dr. M. Vijayalakshmi, Associate Director, PMG welcomed the gathering and Shri E. Mohandas, Convener, STEM-2012 briefed the participants about the STEM series. Plenary lecture on the topic "Magnetron Sputtering of Electronically Active and Passive Layers for Thin Film Solar Cells" was delivered by Dr. Klaus Ellmer of HZB, Germany in which he provided an excellent insight into the structure and various material choices available for fabricating thin film solar cells. The vote of thanks was proposed by Dr. C. Sudha, Secretary STEM-2012.

On the second day plenary lecture was delivered by Dr. H. Murakami of NIMS, Japan on "Effect of Iridium Addition on Oxidation Resistance of coated Ni-based Single Crystal Superalloys". In addition, invited lectures were organized on various topics like sub-surface modification based on plasma based ion implantation and diffusion techniques, Plasma assisted chemical vapour deposition, surface modification and thin film deposition using pulsed lasers, AFM/STM analysis of thin films and coatings and plasma sprayed thermal barrier coatings for molten chloride environment. The theme meeting was attended by around 120 delegates including eminent scientists and research scholars from IITs, NIT, IPR, Anna University and other Engineering/Science colleges, BARC and IGCAR. The technical program was appreciated by the participants and valuable inputs for future theme meetings were provided during the feedback session at the end of the theme meeting.

Reported by E. Mohandas,Convener, STEM-2012

Theme Meeting on Supercritical Fluids
November 20, 2012

Dr. P. R. Vasudeva Rao, Director, CG addressing the participants of the theme meeting on supercritical fluids

The application of supercritical fluid is the subject of growing interest to nuclear and chemical industries, due to environmentally benign and fascinating properties of supercritical fluids. In this context, the southern regional chapter of Indian Association of Nuclear Chemists and Allied Scientists (IANCAS(SRC)), organized a one-day theme meeting on "Supercritical Fluids" on November 20, 2012 sponsored by BRNS at SRI Seminar Hall, Anupuram.

The theme meeting comprised invited lectures on theoretical aspects, physical properties, modelling, instrumentation and applications of supercritical fluids in nuclear and other industries. Dr. T. G. Srinivasan, President, IANCAS(SRC)

inaugurated the meeting. The meeting had two sessions, with four lectures, chaired by Dr. P. R. Vasudeva Rao, Director, CG in the morning session and three lectures in the afternoon, chaired by Dr. T. G. Srinivasan. Eminent speakers from Bhabha Atomic Research Centre, Indian Institute of Science, CSIR and other National laboratories delivered invited lectures. About sixty delegates from various academic and research institutes including ten research fellows participated in the theme meeting. The theme meeting was well received by the delegates and provided good directions on the use of supercritical fluids in nuclear and other industries.

Reported by K. A. Venkatesan, Secretary - IANCAS(SRC)

National Symposium on Radiation Physics
December 12-14, 2012

Indian Society for Radiation Physics (ISRP) organized a three day National Symposium on Radiation Physics (NSRP-19) during December 12-14, 2012 in Mamallapuram. NSRP-19, with a focal theme of "Research and Applications of Radiation Physics: Perspective and Prospective", was supported by Indira Gandhi Centre for Atomic Research, Kalpakkam, Indian Nuclear Society, Kalpakkam Branch, Board of Research in Nuclear Sciences and Atomic Energy Regulatory Board.

During the inaugural function Dr. B. Venkataraman, President, ISRP and Associate Director, RSEG, IGCAR welcomed the gathering and Dr. Prabhat Kumar, Chairman and Managing Director, BHAVINI presided over the function. During his presidential address, he urged the nuclear physicists and design engineers to constantly strive for improvements in the design configuration, optimization of fuel performance and containment of radioactivity.

Shri S. C. Chetal, Director, IGCAR, in his inaugural address stressed the need for the balanced utilization of all forms of energy resources to meet the ever growing energy needs. He also highlighted the consequences of conservative approach to the effects of ionizing radiation which had a bearing on the large safety margins and bias factors adopted in the design of safety related systems and suggested for effective optimization. He also insisted on the need to sharpen the communication skills to effectively reach out the public at large about the facts and figures on nuclear power, safety, environmental releases and the biological effects.

Dr. K. S. Lakshmi, Founder and Principal, Meenakshi College for Women, President, ISRP(K), released the souvenir and the proceedings of NSRP-19. Oration Award in the memory of Dr A. K. Ganguly, formerly Director, Chemistry group, BARC, was conferred on

Theme: Research & Application of Radiation Physics:
Perspective and Prospective

December 12 -14,

Radisson BLU Resort Temple Bay
Mamallapuram, Tamilnadu.

Shri S. C. Chetal, Director, IGCAR, Dr. Prabhat Kumar, Chairman and Managing Director, BHAVINI, Dr. K. S. Lakshmi, Founder and Principal, Meenakshi College for Women, President, ISRP(K), Dr. B. Venkataraman, AD, RSEG, EIRSG and Shri S. Bala Sundar, RSEG during the inaugural session

Shri A. R. Sundararajan, former Director, Safety Research Institute, AERB, Kalpakkam for his outstanding contributions in the field of radiation safety.

The exhibition organized as a part of the conference was formally inaugurated by Shri S. C. Chetal, Distinguished Scientist and Director, IGCAR. Dr. S. Kailas, Director, Physics Group, BARC delivered key note address on "accelerators as a tool for radiation physics and technologies". Dr. D. V. Gopinath, Former Director, Health, Safety and Environment Group, BARC delivered key note address on "some myths about radiation effects and nuclear energy".

The details of the plenary talks delivered at the symposium are summarized below. Prof. G. K. Rath, Chief, Dr. B.R.A Institute-Rotary Cancer Hospital, AIIMS gave a talk on role of ionizing radiation in health care. Shri S.A.V. Satya Murty, Outstanding Scientist, Director, EIRSG, IGCAR delivered a lecture on advances in sensors and instrumentation for radiation detection and measurements. Shri A. R. Sundararajan, Former Director, Safety Research Institute, AERB- pointed out the challenges on assessment of internal exposure from plutonium in his talk. Prof. Rajarajan, Dean, Tamil Nadu Agriculture University, Coimbatore made elaborate presentation on research and applications of ionizing radiation in agriculture sciences. Dr. P. Mohanakrishnan, Former Associate Director, Reactor Physics Group, IGCAR dwelt upon the new research challenges in field of reactor physics and fuel cycle physics during his talk.

There were twenty one technical sessions. Oral presentations and invited talks by eminent scientists from National Institutes and Universities on topics including; Basic radiation processes,

Radiation transport theory and shielding, Radiation related problems at accelerators and reactors, research reactors and AHWRs, Radiation detection and measurements, Radioactivity transport in natural environment and radiation in space, radiation applications in industry, agriculture, food processing and medicine, radiation dosimetric techniques – solid state nuclear track detectors and luminescence and development of nano-phosphors were conducted in parallel sessions.

A total of 189 scientific papers in various topics including, advanced radiation dosimetry, research reactors and applications of radiation in different areas which included agriculture and industries were presented during the conference. There were 109 oral presentations and 80 posters in the technical sessions. Awards for best three oral and poster papers and three young researchers were given away during valedictory on third day of conference. Additionally two more awards were also given to the two best experimental work papers dealing with detection and measurements of radioactivity, which were sponsored by M/s. Nucleonix Ltd, Hyderabad.

The participation by the student community, from basic science and engineering disciplines, in large numbers was one of the highlights of the symposium, which was highly encouraging as pointed out by Dr. D. V. Gopinath in his valedictory address. The collective feedback from the participants was very good. Overall, this was a unique experience for all radiation physicists and a platform for the scientists, young researchers and students of Radiation Physics to share their work, knowledge and observations with each other. This also provided opportunity for the interaction between peer groups in forging collaborative studies.

Reported by Shri S. Bala Sundar, Convenor, NSRP-19

Visit of Dignitaries

Delegation from United States Nuclear Regulatory Commission, USA with Shri S. C. Chetal, Director, IGCAR and senior colleagues of the Centre

A delegation from United States Nuclear Regulatory Commission led by Ms. Kristine Svinicki, Commissioner, US Nuclear Regulatory Commission visited the Centre during October 9-10, 2012. After a meeting with Shri S. C. Chetal, Director, IGCAR and senior colleagues, the delegation visited the Fast Breeder Test Reactor, facilities in Safety Engineering Group, Madras Atomic Power Station and construction site of Prototype Fast Breeder Reactor.

Prof. Vijay Sazawal, Director of Government Programs at USEC Inc. USA, visited the Centre on December 10, 2012. During the meeting with Shri S. C. Chetal, Director, IGCAR and senior colleagues, he briefed about the "Progress in the U.S. Civil Nuclear Program". Prof. Vijay Sazawal then visited the Fast Breeder Test Reactor, Hot cells and Non-Destructive Evaluation Division, facilities in Fast Reactor Technology and Reactor Design Groups and construction site of Prototype Fast Breeder Reactor.

Prof. Vijay Sazawal, Director of Government Programs at USEC, Inc, USA, with Shri S. C. Chetal, Director, IGCAR and Dr. P. R. Vasudeva Rao, Director, CG

Shri Ashok Lavasa, IAS, Additional Secretary (Power), Ministry of Power accompanied by Shri T. S. Sundararajan, GM, NTPC, Shri K. Raj Kumar, Junior Engineer, NTPC and Shri K. N. Babu, ICF, visited the Centre on December 25, 2012. After a meeting with Dr. P. R. Vasudeva Rao, Director, Chemistry Group the delegates visited the Fast Breeder Test Reactor, Madras Atomic Power Station and construction site of PFBR.

Shri Ashok Lavasa, IAS, Additional Secretary (Power), Ministry of Power,   Shri T. S. Sundararajan, General Manager, NTPC, Shri K. Raj Kumar, Junior Engineer, NTPC and Shri K. N. Babu, ICF, with Dr. P.R. Vasudeva Rao, Director, Chemistry Group during their visit to Fast Breeder Test Reactor

Awards & Honours

Shri S. C. Chetal, Distinguished Scientist and Director, IGCAR has been conferred with "Lifetime Achievement Award by the Systems Society of India", in recognition of his illustrious career in systems theory and application and bringing the systems movement to its present day state through his life long contributions to the field.

Shri S.A.V. Satya Murty, Director, Electronics Instrumentation and Radiological Safety Group was awarded "INS Outstanding Service Award" for the year 2011, in recognition of his meritorious scientific and engineering achievements in the field of "Nuclear Reactor Technology, including Reactor Safety".

Shri E. Hemanth Rao, RDG, has received the "INS Young Engineer Award" for the year 2011 for his excellent contribution towards R&D on SFR Safety.

Dr. U. Kamachi Mudali was awarded "Vocational Excellence Award" for the year 2012 by Rotary Club of Chennai Port City, for his outstanding contributions to Nuclear Materials. He has also been elected as "Fellow of NACE" by National Association of Corrosion Engineers (NACE), USA for the year 2013 in view of his outstanding contributions to corrosion science, corrosion engineering and corrosion prevention.

HEPA Filter Test Facility has been accrediated by National Accreditation Board for Testing and Calibration

DAE Awards & Honours

Department of Atomic Energy has instituted annual awards for excellence in Science, Engineering and Technology in order to identify best performers in the area of Research, Technology Development and Engineering in the constituent units (other than Public Sector Undertakings and Aided Institutions). The Young Scientist, Young Engineer, Young Technologist, Homi Bhabha Science and Technology Award and Scientific and Technical Excellence Award fall under this category. Group Achievement awards for recognition of major achievements by groups have also been instituted. Life time Achievement Award is awarded to one who has made significant impact on the DAE's programmes. They are the icons for young scientists and engineers to emulate. The awards consist of a memento, citation and cash prize.

The recipients of the Group Achievement Awards from IGCAR for the year 2012 are:

Homi Bhabha Science and Technology Award	: Dr. D.Ponraju, RDG
Scientific & Technical Excellence Award	: Dr. T.R Ravindran, MSG
	Shri K. Natesan, RDG
Young Scientist Award	: Dr. (Smt.) S. Abhaya, MSG
Young Engineer Award	: Shri D. Naga Sivayya, RDG
Meritorious Award	: Shri J. Selvaraj, ROMG
	Shri P. Swaminathan ROMG
	Shri M.K. Rajappan Achari, ROMG
	Shri M. Sambamurthi, FRTG
	Shri V.K. Parvadeesan, ESG
	Shri P.N. Madhavan, Accounts

Group Achievement Award:

Alpha Tight Transport of High Level Liquid Waste from Reprocessing of FBTR Fuel of 155 GWD/t Burn-up and Partitioning of Minor Actinide in Hot Cell

Dr. P. R. Vasudeva Rao, CG, Group Leader

Dr. M. P. Antony, Dr. N. Sivaraman, Shri K. A. Venkatesan, Smt. S. Rajeswari, Dr. R. Kumaresan, Shri R. Manivannan, Shri A. S. Suneesh, Smt. K. V. Syamala, Shri B. Robert Selvan, Smt. T. Prathibha, Shri R. Karunakaran, Shri T. Kalaiarasu, Shri A. Amalraj, Shri Tippana Bapuji, Shri M. Karunanidhi, Shri S. Sriram, Miss. S. Annapoorani, Shri J. S. Brahmaji Rao, Shri N. Ravi and Shri K. Thiruvengadam from CG, Dr. T. G. Srinivasan, Raja Ramanna Fellow, Chemistry Group, Shri T. Ravi from EIRSG, Shri A. Ravisankar, Shri V. Vijayakumar, Shri D. Natarajan, Shri Surajit Halder, Shri P. Varatharajan, Shri A. Palanivel, Shri S. Somasundaram, Shri P. Ramjee, Shri P. Rameshkumar, Shri K. K. Vinodkumar, Shri Apurba Kumar Majumder, Shri M. D. Mohauddin Ansari, Shri L.Yogananth and Shri Madhusudhana Rao from RpG. The award is also shared by Dr. T. Kumar from KARP, BARC(F).

Design and Development of PFBR Operator Training Simulator

Shri S. A. V. Satya Murty, EIRSG, Group Leader

Ms.T.Jayanthi, Shri K. K. Kuriakose, Shri N. Murali, Shri B. Sasidhar Rao, Dr. S.Srinivasan, Smt. H.Seetha, Shri K. R. S.Narayanan, Smt. Bindu Sankar, Ms. Rashmi Nawlakha, Smt. N. Jasmine, Shri Jaideep Chakraborty, Smt. Tadimeti Lakshmi Priyanka, Shri M. L.Jayalal, Shri R.Jehadeesan, Shri K. Vijayakumar, Smt. T. S. Kavithamani, Shri L.Sathishkumar, Shri G.Shanmugam and Shri B. Subbaraju from EIRSG, Shri P. Selvaraj, Shri K. Madhusoodhanan, Shri N. Theivarajan, Shri K. Natesan, Dr. K. Devan, Shri Jose Varghese, Shri   M. Sivaramakrishna, Shri C.P.Nagaraj, Shri M. Sakthivel, Shri S. Athmalingam, Shri S. Raghupathy, Shri A. Venkatesan, Shri R. R. Ramanarayanan, Shri U. Parthasarathy, Shri Tanmay Vasal and Smt. T.Sathyasheela from RDG.

Thermal Shock Test Facility

Shri B. K. Sreedhar, FRTG, Group Leader

Shri Shiv Prakash Ruhela, Shri Sudheer Patri, Shri S. Chandramouli, Shri P. Madan Kumar, Shri Rakesh Kumar Mourya, Shri S. Ignatius Sundar Raj, Smt. S. Nagajothi, Shri R. Rajendra Prasad, Shri Nilayendra Chakraborty, Shri J. Prabhu, Shri A. Kolanjiappan, Shri R. Ramalingam, Shri R. Krishnnamurthy, Shri M. Sambamurthi, Shri P. Varadan, Shri R. Punniyamoorthy, Shri K. Karunakaran, Shri R. Shanmugam, Shri C. Adikesavan, Shri M. T. Janakiraman, Shri N. Mohan, Shri K. Arumugam, Shri Parmanand Kumar, Shri J. Prabhakaran, Shri P. C. V. Murugan, Shri N. Sreenivas, Shri L. Eagambaram, Shri P. R. Ashok Kumar, Shri M. Karthikeyan, Shri K. Ramesh, Shri V. Kumaraswamy, Shri Shaik Rafee, Shri K. Ganesh, Shri Ashish Tiwari, Shri L. Mohanasundaram, Shri L. Muthu, Shri T. V. Maran, Smt. J. I. Sylvia, Shri P. Vijayamohanarao, Shri M. Anbuchelian, Shri P. Bakthavatchalam, Shri C. Ambujakshan Nair, Shri A. Kulanthi, Smt. S. Narmadha, Shri G. Vijayakumar, Shri R. Iyappan, Shri Sarat Kumar Dash, Shri D. K. Saxena, Shri K. Radhakannan and Shri R. Parandaman from FRTG.

Development of Oxide Dispersion Strengthened 9Cr Ferritic -Martensitic Steel Cladding Tubes for Sodium Cooled Fast Breeder Reactors

Shri T. Jayakumar, MMG, Group Leader

Dr. M. D. Mathew, Dr. Saroja Saibaba, Dr. K. Laha, Dr. B. P. C. Rao, Shri E. Mohandas, Dr. U. Kamachi Mudali, Dr. Divakar Ramachandran, Dr. N. Parvathavarthini, Dr. Arup Dasgupta, Dr. Anish Kumar, Dr. K. V. Rajkumar, Ms. Diptimayee Samantaray, Shri Ram Kishor Gupta, Shri S. Thirunavukkarasu, Smt. K.S.Chandravathi, Shri M. Nandagopal, Shri G. V. Prasad Reddy, Shri Chanchal Ghosh and Shri Pradyumna Kumar Parida from MMG. The award is also shared by Shri B. Lakshmi Narayana, Shri B. Prahlad, Shri C. Phani Babu, Dr. Komal Kapoor, Shri S.K. Jha, Shri G. N. Ganesha, Shri L. Sudersanam, Shri Pranay Kumar Maity, Shri K. Umamaheswara Rao, Shri K. Ravikrishna, Shri Ch. Sampath Kumar Chary, Shri K. Somasekhar Reddy, Shri D. Sambasiva Rao, Shri P. Yadagiri, Shri G. Narayana Reddy and Shri M. A. Rasheed from NFC, Hyderabad.

Ferroboron as In-vessel Shield Material in Fast Breeder Reactors

Dr. R.S. Keshavamurthy, ROMG, Group Leader

Shri D. Sunil Kumar, Shri D. Venkata Subramanian, Shri Adish Haridas, Shri V. Rajan Babu and Shri S. Clement Ravi Chandar from RDG, Shri Raju Subramanian, Shri Arun Kumar Rai, Dr. S. Murugan, Shri K. A. Gopal, Shri M. Muthu Ganesh, Shri Rajesh Saxena, Shri R. Ramesh, Shri C. N. Venkiteswaran, Shri D. Ganesan and Shri V. Anandaraj from MMG, Dr. S. Anthonysamy, Dr. K. Chandran, Dr. R. Sudha and Smt. P. R. Reshmi from CG, Dr. V. Ganesan from ROMG and Shri N. Vijayan Varier from TC&QCD

Main Vessel - Roof Slab Weld Joint Mock up for PFBR Project

Shri R. Sritharan, RDG, Group Leader

Shri Gagan Gupta, Shri V. Rajan Babu, Shri Sriramchandra Aithal, Shri P. Puthiyavinayagam, Shri Abhishek Mitra, Shri C. Raghavendran, Shri Ravi Prakash Pandey, Shri Kulbir Singh, Shri V. Sebasti John, Shri S. Saravanan, Smt. P. Swetha, Shri G. Venkataiah, Shri S. K. Rajesh, Shri M. Babu Rao, Shri R. Manu, Shri V. Devaraj and Shri G. Soundararajan from RDG, Dr. B. Venkataraman, Shri P. Jagannathan, Shri B. Ananadapadmanaban, Shri G. Ramesh, Smt. Alka Kumari, Shri Shrikrishna Tripathi, Shri Sukumar Manna and Shri P. Narayana Rao from EIRSG and Dr. Shaju K. Albert and Shri Harish Chandra Dey from MMG

Indigenous Repair and Servicing of HPGe detectors

Shri J. Jayapandian, MSG, Group Leader

Shri C. R. Venkata Subramani, Shri G. Gunasekaran from CG, Shri R. Bhaskaran, Smt. O. K . Sheela, Shri   A. V, Thanikai Arasu, Shri   N. Chinnasamy from MSG, Shri G. Kempulraj, Shri   P. Shanmugam, Shri P. Karruppasamy, Shri K. M. Natarajan and Shri N. Lakshimipathi from ESG(E&M), Shri R. Mathiyarasu, Shri   M. K. Sundararajan, Shri   Patil Sunil Waman from EIRSG and Shri P. C. Sandheep from RpG. The award is also shared by Dr. K. G. Bhushan, Dr. V. B. Chandratre,   Dr. V. D. Srivastava, Shri Uday Sanjay Sule and Shri Sunil M. Rodrigues from BARC.

Couroubita guanensis (Canon ball tree)